**MINISTÉRIO DA EDUCAÇÃO**
**UNIVERSIDADE FEDERAL DO RIO GRANDE DO NORTE**
**CENTRO DE CIÊNCIAS DA SAÚDE**
**PROGRAMA DE PÓS-GRADUAÇÃO EM CIÊNCIAS DA SAÚDE**

# Nanoemulsão estabilizada por hidrofobina, um carreador promissor para nutracêuticos.

**Christian Melo de Oliveira**

**NATAL/RN**
**2018**

**Christian Melo de Oliveira**

# Nanoemulsão estabilizada por hidrofobina, um carreador promissor para nutracêuticos.

Dissertação apresentada ao Programa de Pós-Graduação em Ciência da Saúde da Universidade Federal do Rio Grande do Norte como requisito para a obtenção do título de Mestre em Ciências da Saúde.

Orientador: Prof. Dr. Eryvaldo Sócrates Tabosa do Egito

Coorientador: Dr. Francisco Humberto Xavier Júnior

**NATAL/RN**
**2018**

Universidade Federal do Rio Grande do Norte - UFRN
Sistema de Bibliotecas - SISBI
Catalogação de Publicação na Fonte. UFRN - Biblioteca Setorial do Centro Ciências da Saúde - CCS

Oliveira, Christian Melo de.
Nanoemulsão estabilizada por hidrofobina, um carreador promissor para nutracêuticos / Christian Melo de Oliveira. - 2018.
61f.: il.

Dissertação (Mestrado) - Universidade Federal do Rio Grande do Norte, Centro de Ciências da Saúde, Programa de Pós-Graduação em Ciências da Saúde. Natal, RN, 2018.
Orientador: Eryvaldo Sócrates Tabosa do Egito.
Coorientador: Francisco Humberto Xavier Júnior.

1. Nanoemulsão - Dissertação. 2. Hidrofobina - Dissertação. 3. Óleo de copaíba - Dissertação. 4. HFBII - Dissertação. 5. Nutracêutico - Dissertação. I. Egito, Eryvaldo Sócrates Tabosa do. II. Xavier Júnior, Francisco Humberto. III. Título.

RN/UF/BS-CCS CDU 615.451.2

Elaborado por ANA CRISTINA DA SILVA LOPES - CRB-15/263

**MINISTÉRIO DA EDUCAÇÃO**
**UNIVERSIDADE FEDERAL DO RIO GRANDE DO NORTE**
**CENTRO DE CIÊNCIAS DA SAÚDE**
**PROGRAMA DE PÓS-GRADUAÇÃO EM CIÊNCIAS DA SAÚDE**

Coordenadora do Programa de Pós-graduação em Ciências da Saúde
Prof.ª Dra. Ana Katherine da Silveira Gonçalves de Oliveira

**Christian Melo de Oliveira**

**Nanoemulsão estabilizada por hidrofobina, um carreador promissor para nutracêuticos.**

**Aprovado em 22/10/2018**

**Banca examinadora:**

Presidente da banca: Prof. Dr. Eryvaldo Sócrates Tabosa do Egito - UFRN

Membros da banca: Prof. Dr. Ádley Antonini Neves de Lima - UFRN

Prof. Dr. Elquio Eleamen Oliveira - UEPB

## AGRADECIMENTOS

Agradeço, inicialmente, a Deus por me permitir ter fé, saúde e a minha família a todo o momento. Agradeço aos meus pais, Oliveira e Francisca, pelos ensinamentos da vida. Agradeço ao Prof. Dr. Sócrates e ao Dr. Humberto pela confiança em mim depositada. Agradeço aos demais profissionais que contribuíram para a execução do projeto. Finalmente, agradeço aos amigos que me apoiaram e participaram do meu crescimento profissional.

## RESUMO

A hidrofobina II (HFBII) é um biopolímero anfifílico que poderia ser explorado para estabilizar nanoemulsões de estrutura óleo-água como um sistema carreador de nutracêuticos. O objetivo desse estudo foi produzir sistemas nanoemulsionados de estruturas óleo-água, estabilizados por HFBII, através de um processo de emulsificação espontânea, utilizando o óleo de copaíba como componente bioativo da formulação. A HFBII foi obtida a partir do cultivo de uma cepa selvagem de *Trichoderma reesei*, utilizando a técnica de extração proteica com $CO_2$ e isolamento por RP-HPLC. A proteína intacta, obtida através do isolado proteico, e os seus peptídeos foram identificados por análises de espectrometria de massa, enquanto que o grau de pureza proteico foi determinado por medidas de tensão superficial. Um planejamento fatorial completo $2^3$ com três pontos centrais foi usado para a obtenção de um sistema nanoemulsionado ótimo, cujas propriedades físico-químicas foram estudadas sob diferentes condições de força iônica e pH. O resultado da espectrometria de massa da proteína intacta mostrou um único pico de, aproximadamente, 7.000 Da, enquanto que a avaliação da similaridade peptídica identificou 6 fragmentos de íons que estão presentes no banco de dados da HFBII. O isolado da HFBII apresentou um aumento no fator de purificação de 3,2 vezes, quando comparado à fração do sobrenadante do meio de cultura. A obtenção de um sistema nanoemulsionado ótimo foi alcançada com o uso dos menores níveis das variáveis independentes (0,005% $_{(m/m)}$ de HFBII, 0,02% $_{(m/m)}$ de óleo de copaíba e 10% $_{(v/v)}$ de proporção de fase orgânica para aquosa). O sistema nanoemulsionado ótimo apresentou um tamanho de gotícula nanométrico (<200 nm), uma estreita distribuição de tamanho (PDI <0,2) e um potencial zeta de ≈ -30 mV, o qual se manteve estável em baixas concentrações de NaCl (≤ 25 mM) e pH próximo à neutralidade. Estes resultados demonstraram a viabilidade do uso da HFBII como biopolímero para estabilizar sistemas nanoemulsionados. Além disso, o sistema nanoemulsionado estabilizado por HFBII é um carreador promissor para nutracêuticos em aplicações de tecnologia de alimentos.



Palavras-chave: Hidrofobina, HFBII, óleo de copaíba, nanoemulsão, nutracêutico.

## ABSTRACT

Hydrophobin II (HFBII) is an amphiphilic biopolymer that could be explored to stabilize oil-in-water nanoemulsions as nutraceutical delivery systems. This study reports the production of HFBII-stabilized nanoemulsions by a spontaneous emulsification process using copaiba oil as a bioactive lipid. HFBII was isolated from a wild-type *Trichoderma reesei* and characterized. A $2^3$ full factorial design with three central points was used to obtain an optimal nanoemulsion system, whose physical-chemical properties were studied under different ionic strength and pH. The peptide similarity search allowed the identification of a series of 6 ion fragments from the isolated fraction, which can be attributed to the amino acid sequences of the HFBII database. The optimal nanoemulsion system presented a nanoscale droplet size (<200 nm), a narrow size distribution (PDI <0.2) and a zeta potential of ≈ -30 mV, which was stable at low salt content and pH values close to the neutrality. These results demonstrated the feasibility of using HFBII as a biopolymer to stabilize nanoemulsion systems. Furthermore, the HFBII-stabilized nanoemulsion is a promising carrier for nutraceuticals in food technology applications.



Keywords: Hydrophobin, HFBII, copaiba oil, nanoemulsion, nutraceutical.

## LISTA DE ABREVIATURAS E SIGLAS

**AFM**- Microscopia de força atômica;

**ANOVA**- Análise de variância;

**BCA**- Ácido bicinconínico;

**BSA**- Albumina de soro bovino;

**CCT**- Coleção de Culturas Tropical;

**HFBII**- Hidrofobina II;

**MALDI-TOF/TOF**- Ionização e dessorção a laser assistida por matriz-tempo de voo/ tempo de voo;

**MEV**- Microscopia eletrônica de varredura;

**PDI**- Índice de polidispersividade;

**RP-HPLC**- Cromatografia líquida de alta eficiência em fase reversa;

**SDS-PAGE**- Eletroforese em gel de poliacrilamida-dodecil sulfato de sódio;

$\gamma_0$- Tensão superficial inicial;

$\gamma$- Tensão superficial;

$\Pi$- Pressão de superfície.

## LISTA DE FIGURAS

## LISTA DE TABELAS

**SUMÁRIO**

## 1 INTRODUÇÃO

O uso de biopolímeros na indústria de alimentos é uma abordagem tecnológica, amplamente, explorada para o desenvolvimento de sistemas carreadores (1). Os biopolímeros têm propriedades intrínsecas excepcionais, como a habilidade para formar filmes interfaciais (2), biofuncionalidade/biocompatibilidade (3), biodegradabilidade (4) e bioatividade (5).

As proteínas são biopolímeros que constituem diversos materiais de origem biológica, e que podem ser encontrados na forma de produtos do metabolismo celular de micro-organismos. Proteínas de origem microbiana possuem estruturas anfifílicas e, consequentemente, propriedade tensoativa, e são classificadas com base no organismo produtor e constituição química (6). Produtos de baixa e elevada massa molecular são responsáveis por diversas funções biológicas promovidas pela alta capacidade de redução da tensão de interfaces: aumento da área superficial e solubilidade aparente de substratos insolúveis em água; adesão às superfícies e formação de estruturas aéreas (ex., hifas, corpos de frutificação) (7).

As hidrofobinas são pequenas proteínas globulares (7-15 kDa) produzidas por fungos filamentosos (8). Suas estruturas primárias são caracterizadas pela presença de oito resíduos de cisteína, os quais formam quatro pontes dissulfeto que estabilizam as diversas formas proteicas (9). A exposição permanente das suas regiões hidrofóbicas, assim como a formação de dímeros anfifílicos, são os fatores determinantes à sua elevada atividade interfacial (9). Baseando-se no perfil hidropático, duas classes de hidrofobinas são definidas: classe I e II compostas por moléculas de alta e baixa hidrofobicidade, respectivamente (9).

A hidrofobina II (HFBII) pertence à classe II, a qual é produzida pelo fungo filamentoso *Trichoderma reesei* e difundida para o meio de cultura e superfície de esporos (8, 9). Sua estrutura *β*-barril de domínio único tem uma região hidrofílica formada por pares de filamentos *β* antiparalelos e uma *α*-hélice. A superfície hidrofóbica da HFBII é formada por estruturas alifáticas de resíduos de aminoácidos localizados nos filamentos *β* e na região N-terminal (9). Os monômeros e dímeros anfifílicos da proteína agem na formação de filmes interfaciais, possibilitando avaliar o seu potencial na estabilização de sistemas emulsionados (9).

Emulsão e nanoemulsão são sistemas coloidais formados por duas fases imiscíveis, as quais são estabilizadas por tensoativos na forma de gotículas

dispersas em uma fase contínua (10). Estruturalmente, os sistemas emulsionados simples podem ser classificados em dois tipos: gotículas de óleo dispersas em água (óleo-água); ou gotículas de água dispersas em óleo (água-óleo) (10). A nanoemulsão possui instabilidade termodinâmica, apesar de ser formada por gotículas de tamanho nanométrico, cujo processo de separação de fases é favorecido por ter uma menor energia livre. Porém, a formação de barreiras energéticas interfaciais pode fornecer estabilidade cinética a esse sistema, prolongando o tempo de dispersão de suas gotículas metaestáveis (10).

As proteínas estabilizam sistemas emulsionados através da formação de filmes viscoelásticos que reduzem a tensão interfacial, promovem resistência mecânica e geram forças repulsivas nas superfícies das gotículas (2). O desenvolvimento de nanoemulsões estabilizadas por proteínas tem sido explorado com o uso de óleos bioativos para a formação de compartimentos oleosos nutracêuticos (11). O óleo-resina de copaíba, proveniente de árvores do gênero *Copaifera* spp., tem uma ampla gama de propriedades biológicas (ex., anti-inflamatória, antimicrobiana) atribuídas à sua mistura complexa de sesquiterpenos e diterpenos (12). A formulação de um sistema nanoemulsionado estabilizado por HFBII, utilizando o óleo de copaíba como molécula bioativa, poderia ter uso potencial na indústria de alimentos (13).

O conhecimento dos parâmetros de formulação é fundamental para o aprimoramento das propriedades físico-químicas de sistemas coloidais estabilizados por proteínas (14). Os processos de emulsificação influenciam, diretamente, no tamanho de gotícula final. Esses processos podem ser classificados como técnicas de baixa energia, as quais são dependentes da formulação, ou de alta energia, as quais são dependentes do dispositivo de agitação (15). A técnica de emulsificação espontânea é um processo de baixa energia bastante explorado por não ser agressivo às moléculas sensíveis, como as proteínas (15). Além do processo de emulsificação, a composição da fase aquosa (ex., força iônica, pH) pode afetar a estabilidade de sistemas emulsionados através de modificações no filme interfacial proteico (16).

# 2 OBJETIVOS

## 2.1 Objetivo geral

O objetivo desse estudo foi produzir sistemas nanoemulsionados de estruturas óleo-água, estabilizados por HFBII, através de um processo de emulsificação espontânea, utilizando o óleo de copaíba como componente bioativo da formulação.

## 2.2 Objetivos específicos

- Isolar a HFBII de cepa selvagem de *Trichoderma reesei* QM9414, e caracterizá-la;
- Determinar a composição ótima do sistema nanoemulsionado, utilizando uma abordagem de planejamento fatorial;
- Determinar os efeitos de eletrólitos nas propriedades físico-químicas do sistema nanoemulsionado ótimo.

## 3 JUSTIFICATIVA

Diversos tipos de sistemas carreadores são elaborados para melhorar características intrínsecas aos diferentes tipos de moléculas bioativas (ex., baixa solubilidade, hidrólise, degradação enzimática/oxidativa) (13). (Malmsten, 2006)(Malmsten, 2006)(Malmsten, 2006)(Malmsten, 2006)(Malmsten, 2006)(Malmsten, 2006)(Malmsten, 2006)A nanoemulsão é um tipo de carreador utilizado no transporte, no aumento da biodisponibilidade e na liberação controlada de moléculas bioativas devido ao seu tamanho de gotícula reduzido e à sua estabilidade cinética (10).

O uso de proteínas no desenvolvimento de sistemas nanoemulsionados confere propriedades estruturais favoráveis à biodistribuição de moléculas bioativas: a estruturação de monocamada proteica nas superfícies das gotículas diminui a evasão e aumenta a estabilidade das moléculas incorporadas (14); a degradação de materiais biopoliméricos em tecidos-alvo promove a formação de produtos de baixa toxicidade ao organismo (3). As hidrofobinas se diferenciam das demais proteínas por terem estruturas de elevada ação tensoativa e resistência às altas temperaturas (≈ 60 ºC), além de sofrerem leve mudança conformacional em interfaces (8, 9).

O uso de óleos naturais bioativos, como o óleo-resina de copaíba (*Copaifera langsdorffii*), confere propriedades biológicas aos sistemas emulsionados, nos quais compartimentos oleosos de estrutura óleo-água poderiam ser estabilizados por proteínas (11, 17). Assim, a dispersão oleosa doaria ao sistema propriedades biológicas, além de agir como reservatório de moléculas lipossolúveis (17). Portanto, as propriedades intrínsecas aos biopolímeros (ex., HFBII) e aos óleos naturais (ex., óleo de copaíba) favorecem os estudos de desenvolvimento de sistemas emulsionados.

# 4 MÉTODOS

## 4.1 Condições de cultura fúngica

A cepa de *T. reesei* QM9414 foi cultivada em incubadora com agitação orbital (TE-420®, Tecnal, Brasil) programada a 200 rpm e 25 ºC, como descrito por Khalesi et al. (18). A HFBII foi produzida em frascos de 500 mL contendo um meio de cultura (120 mL) composto por lactose como fonte de carbono (18). O pH final do meio de cultura foi ajustado para o valor de 4,5, usando 10% $_{(v/v)}$ de $H_3PO_4$. A cinética de crescimento da *T. reesei* foi analisada, manualmente, por nefelometria (HI 98703®, Hanna Instruments, Itália) durante 7 dias de cultura, utilizando a dispersão de biomassa micelial em água ultrapura na razão 1:10. O sobrenadante rico em proteína foi coletado no quarto dia de cultura, no qual o meio líquido foi centrifugado (Gusto®, Fisherbrand, EUA) a 8.000 *g* por 25 min.

## 4.2 Purificação e caracterização da HFBII

A técnica de extração proteica com $CO_2$ foi usada para obter a fração rica em HFBII (18). A HFBII foi isolada por RP-HPLC analítico (ÄKTApurifier®, Amersham Biosciences, Suíça) (coluna 15 RPC®, 3 mL; GE Healthcare, EUA) com gradiente de eluição de acetonitrila 0-60%, contendo 0,1% de ácido trifluoroacético, na razão de fluxo de 2 $mL.min^{-1}$ e detecção UV a 214 nm (18). O solvente orgânico foi removido por evaporador rotativo (RV 10® basic, IKA, Alemanha) a 25 ºC. O pH final da solução proteica foi ajustado para o valor de 7,4, usando NaOH a 1 N. Frações proteicas foram coletadas de todas as etapas para as análises de quantificação e caracterização. O conteúdo proteico foi determinado pelo método do ácido bicinconínico (BCA), utilizando um kit de ensaio (Pierce®, Thermo Scientific, EUA), no qual albumina do soro bovino (BSA) foi usada como padrão (19). O grau de pureza da HFBII foi analisado por tensão superficial ($\gamma$) (Seção 4.6.1), no qual o mesmo volume foi coletado, a partir das frações de purificação, e diluído com água ultrapura (0,01% $_{(m/m)}$ sobrenadante, 0,008% $_{(m/m)}$ extrato ($CO_2$) e 0,002% $_{(m/m)}$ isolado (RP-HPLC)). Os resultados foram expressos, numericamente, através da pressão de superfície ($\Pi$) ($\Pi = \gamma_0 - \gamma$).

4.2.1 Eletroforese em gel de poliacrilamida-dodecil sulfato de sódio (SDS-PAGE)

As frações proteicas foram analisadas por SDS-PAGE (SE 600 Ruby®, Amersham Biosciences, Suíça), a qual foi realizada em gel homogêneo de poliacrilamida a 15% (19). As amostras foram preparadas como descrito por Araújo et al. (19). O marcador molecular foi usado na faixa de 6,5-200 kDa (SigmaMarker®, Sigma-Aldrich, EUA), e as bandas proteicas foram coradas com prata (20).

4.2.2 Espectrometria de massa

A identificação da proteína intacta foi realizada por MALDI-TOF-MS (Autoflex III®, Bruker Daltonik, Alemanha). O espectro de massa foi obtido na faixa de 2000-20000 Da, e na frequência de 47 Hz. Um padrão proteico (Bruker Daltonik, Bremen, Alemanha) foi utilizado como calibrador externo: insulina ($[M+H]^+$ 5734,51 m/z), citocromo C ($[M+2H]^{2+}$ 6180,99 m/z), mioglobina ($[M+2H]^{2+}$ 8476,65 m/z), ubiquitina ($[M+H]^+$ 8565,76 m/z), citocromo C ($[M+H]^+$ 12360,97 m/z) e mioglobina ($[M+H]^+$ 16952,30 m/z). A identificação dos peptídeos foi realizada por MALDI-TOF MS/MS na frequência de 100 Hz e faixa de 1000-8040 Da, usando BSA (Sigma-Aldrich, St. Louis, EUA) como calibrador interno. As aquisições foram feitas no modo de reflexão de íons positivos. Os íons foram acelerados em 20 kV. As amostras foram preparadas como descrito por Khalesi et al. (5). Sucintamente, a amostra (1 µL) foi depositada na placa de análise (MTP 384® ground steel, Bruker Daltonik, Alemanha) e misturada com a solução matriz (1 µL). Na pesquisa de similaridade peptídica, o programa *Fragment Ion Calculator*® (Proteomics Toolkit) foi usado para comparar os fragmentos de íons observados com o banco de dados da HFBII *UniProt* (ID P79073).

## 4.3 Produção dos sistemas nanoemulsionados

Os sistemas nanoemulsionados de estrutura óleo-água foram produzidos por emulsificação espontânea (21, 22). A fase aquosa foi composta por HFBII (0,005, 0,0175 e 0,030% $_{(m/m)}$) em água ultrapura, enquanto que a fase orgânica foi preparada com óleo de copaíba (0,02, 0,06 e 0,10% $_{(m/m)}$) em acetona. Os tubos de vidro contendo a fase aquosa foram sonicados em banho de ultrassom (USC-

1800A®, UNIQUE, Brasil) por 1 min para dispersar os agregados proteicos e remover pequenas bolhas. Em seguida, a fase orgânica (100 µL) foi, lentamente, injetada na fase aquosa (1 mL) sob agitação magnética (C-MAG HS 7®, IKA, EUA) a 750 rpm e 25 ºC. Para a completa evaporação da acetona, as amostras foram aquecidas (ETS D5®, IKA, EUA) a 50 ºC por 60 min sob moderada agitação magnética. Após 24 h, as análises físico-químicas das nanoemulsões foram realizadas.

### 4.4 Planejamento fatorial

Uma abordagem de planejamento fatorial completo $2^3$ com três pontos centrais foi usada para obter o sistema nanoemulsionado ótimo, no qual foi requerido um total de 11 experimentos. As amostras foram preparadas como descrito na Seção 4.3, usando as concentrações de HFBII (0,005, 0,0175, 0,030% $_{(m/m)}$), de óleo de copaíba (0,02, 0,06, 0,10% $_{(m/m)}$) e as proporções de fase orgânica para aquosa (10, 30, 50% $_{(v/v)}$) como variáveis independentes. Os fatores, tamanho de gotícula, índice de polidispersividade (PDI) e potencial zeta foram selecionados como variáveis dependentes. O planejamento fatorial foi utilizado para a obtenção de nanoemulsões de pequeno tamanho de gotículas de carga negativa. As análises estatísticas foram feitas com o uso do programa *Statistica*® (Versão 7.0, StatSoft Inc., EUA). Os gráficos de superfície de resposta foram gerados para a visualização simultânea dos efeitos de cada variável nos parâmetros de resposta.

### 4.5 Influência da força iônica e do pH na nanoemulsão estabilizada pela HFBII

Os efeitos de eletrólitos nas propriedades físico-químicas do sistema nanoemulsionado ótimo, selecionada com base no planejamento fatorial da Seção 4.4, foram analisados durante 7 dias. Inicialmente, a força iônica na fase aquosa foi ajustada para 25, 250 ou 500 mM de NaCl, e o pH mantido em 7,4. Nos experimentos seguintes, o pH da fase aquosa foi ajustado para os valores de 2, 6, 7,4 ou 10 (MPT-2®, Malvern, Reino Unido), utilizando uma solução de HCl a 1 N ou NaOH a 1 N, e a força iônica mantida nos menores valores (<25 mM NaCl). A composição da fase aquosa foi modificada antes da produção dos sistemas nanoemulsionados. As caracterizações físico-químicas foram realizadas para

estabelecer uma correlação entre a composição da fase aquosa e a estabilidade da nanoemulsão.

## 4.6 Análises físico-químicas

### 4.6.1 Análises de gota pendente

A tensão superficial ($\gamma$) dinâmica foi obtida por medidas do relaxamento de gotas em função do tempo, usando o equipamento *Contact-Angle-Drop-Shape-Analysis System 100*® (Krüss, Alemanha) com o programa DSA3®. As gotas foram formadas por uma microseringa acoplada a um motor, usando uma agulha de aço inoxidável. As medidas foram realizadas em intervalos de tempo de 5 s, analisando o formato das gotas com uma câmera de alta resolução (25 imagens por segundo). A tensão superficial de 0,002% $_{(m/m)}$ de HFBII em água ultrapura foi avaliada após os ajustes da força iônica e do pH da fase aquosa.

### 4.6.2 Espalhamento dinâmico de luz

O diâmetro hidrodinâmico e a distribuição de tamanho dos sistemas nanoemulsionados foram medidos pelo *Zetasizer Nano-ZS*® (Malvern, Reino Unido). As nanoemulsões foram diluídas para uma concentração aproximada de 0,0025% $_{(m/m)}$ em água ultrapura, e introduzidas em cubeta de poliestireno (DTS0012®, Malvern, Reino Unido). As medidas foram realizadas a 25 ºC, usando um ângulo de detecção de 173º, um índice de refração de 1,33 para o meio de dispersão e 1,45 para o sistema nanoemulsionado, e uma viscosidade de 0,89 cP para o meio de dispersão.

### 4.6.3 Potencial zeta

O potencial zeta dos sistemas nanoemulsionados foi medido (Zetasizer Nano-ZS®, Malvern, Reino Unido) através das amostras e parâmetros de medidas, anteriormente, descritos para a análise de espalhamento dinâmico de luz. A constante dielétrica usada para o meio de dispersão foi de 78,5. Uma célula capilar (DTS1070®, Malvern, Reino Unido) foi usada para as análises de potencial zeta.

4.6.4 Microscopia de força atômica (AFM)

As micrografias do filme de HFBII foram obtidas por AFM no microscópio *SPM-9700*® (Shimadzu, Japão), operando no modo de contato intermitente em temperatura ambiente. As amostras contendo 0,002% $_{(m/m)}$ de HFBII em água ultrapura foram espalhadas em superfície de mica e secas em temperatura ambiente durante 48 h. Os *cantilevers* de silicone (Pointprobe®, NanoWorld AG, Suíça) foram utilizados para obter as imagens, usando uma constante de mola na faixa de 21-78 N/m. A frequência de ressonância foi ajustada para 320 kHz, e a taxa de escaneamento foi de 1 Hz. Uma área de 5 µm x 5 µm foi analisada para cada amostra.

4.6.5 Microscopia eletrônica de varredura (MEV)

A morfologia das gotículas do sistema nanoemulsionado estabilizado por HFBII foi analisada no microscópio *SEM EVO LS15*® (Carl Zeiss, Alemanha) com uma voltagem de aceleração de 10 kV. As amostras (10 µL) foram depositadas em superfícies de vidro, secadas em temperatura ambiente e recobertas com ouro (Q150T ES®, Quorum Technologies, Reino Unido) para evitar o carregamento sob o feixe de elétrons e para aumentar o contraste da imagem.

## 4.7 Análises estatísticas

A maioria dos experimentos foi feita em duplicata, e os resultados expressos como a média ± D.P. As médias de dois grupos foram comparadas através do teste t de Student não pareado. Quando múltiplos grupos foram comparados, a análise de variância (ANOVA) unidirecional foi usada com as comparações múltiplas de Tukey. Os dados estatísticos foram considerados significativos em *p*-valores <0,05. Os programas *GraphPad Prism*® (Versão 5.0, GraphPad Software Inc., EUA) e *Statistica*® (Versão 7.0, StatSoft Inc., EUA) foram usados para as análises estatísticas dos dados.

## 5 ARTIGO PRODUZIDO

**5.1** O artigo *Hydrophobin-stabilized nanoemulsion produced by a low-energy emulsification process: a promising carrier for nutraceuticals* foi aceito no periódico *Food Hydrocolloids* que possui fator de impacto 5.089 e Qualis A1 da CAPES para a área Medicina ll.

# Hydrophobin-stabilized nanoemulsion produced by a low-energy emulsification process: a promising carrier for nutraceuticals

Christian Melo de Oliveira[a], Francisco Humberto Xavier Júnior[b], Andreza Rochelle do Vale Morais[a], Iasmim Lopes de Lima[b], Roberto Afonso da Silva[b], André Ezequiel Gomes do Nascimento[c], Nathália Kelly de Araújo[d], Mariane Cajuba de Britto Lira Nogueira[b], Arnóbio Antônio da Silva Júnior[d], Matheus de Freitas Fernandes Pedrosa[d], Eryvaldo Sócrates Tabosa do Egito[a,*]

[a]Laboratório de Sistemas Dispersos, Departamento de Farmácia, Universidade Federal do Rio Grande do Norte – UFRN, Rua General Gustavo Cordeiro de Faria, 59012-570, Natal, RN, Brazil. (christian_melo6@hotmail.com, andrezarochelle@hotmail.com)

[b]Laboratório de Imunopatologia Keizo Asami (LIKA), Universidade Federal de Pernambuco – UFPE, Av. Professor Moraes Rego, 50670-900, Recife, PE, Brazil. (ffhxjunior@yahoo.com.br, minklopes@gmail.com, robafonso@hotmail.com, marianelira@gmail.com)

[c]Núcleo de Ensino e Pesquisa em Petróleo e Gás II, Departamento de Engenharia Química – UFRN, Av. Senador Salgado Filho, 59072-970, Natal, RN, Brazil. (andrenascimento.eq@gmail.com)

[d]Laboratório de Tecnologia e Biotecnologia Farmacêutica, Departamento de Farmácia – UFRN, Rua General Gustavo Cordeiro de Faria, 59012-570, Natal, RN, Brazil. (nakar_rn@hotmail.com, arnobiosilva@gmail.com, mffpedrosa@gmail.com)

*** Corresponding author:**

Professor Eryvaldo Sócrates Tabosa do Egito, PhD

Rua Praia de Areia Branca, 8448. Ponta Negra, Natal – Brazil (59094-450)

Phone: +55 84 99431 8816 or +55 84 3342 9817

E-mail address: socratesegito@gmail.com

## Highlights

- $CO_2$ extraction successfully concentrated the HFBII, which was isolated by RP-HPLC.
- 6 ion fragments were found on the isolated HFBII.
- Nanoemulsion presented small droplet size, narrow PDI and highly negative charge.
- The low content of copaiba oil improved the mechanical disruption of oil droplets.
- Nanoemulsion was stable at low salt content and pH values close to the neutrality.

## Graphical abstract

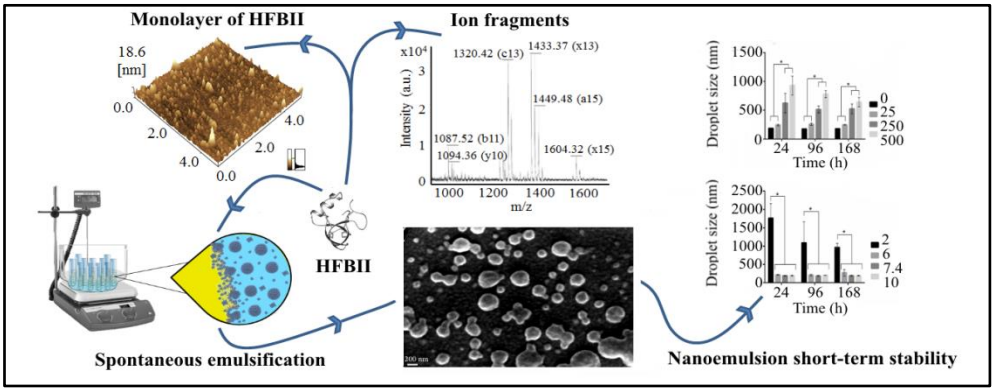

**Abstract**

Hydrophobin II (HFBII) is an amphiphilic biopolymer that could be explored to stabilize oil-in-water nanoemulsions as nutraceutical delivery systems. This study reports the production of HFBII-stabilized nanoemulsions by a spontaneous emulsification process using copaiba oil as a bioactive lipid. HFBII was isolated from a wild-type *Trichoderma reesei* and characterized. A $2^3$ full factorial design with three central points was used to obtain an optimal nanoemulsion system, whose physical-chemical properties were studied under different ionic strength and pH. The peptide similarity search allowed the identification of a series of 6 ion fragments from the isolated fraction, which can be attributed to the amino acid sequences of the HFBII database. The optimal nanoemulsion system presented a nanoscale droplet size (<200 nm), a narrow size distribution (PDI <0.2) and a zeta potential of ≈ -30 mV, which was stable at low salt content and pH values close to the neutrality. These results demonstrated the feasibility of using HFBII as a biopolymer to stabilize nanoemulsion systems. Furthermore, the HFBII-stabilized nanoemulsion is a promising carrier for nutraceuticals in food technology applications.

**Keywords:** Hydrophobin, HFBII, copaiba oil, nanoemulsion, nutraceutical.

## Abbreviation list

**AFM**- Atomic force microscopy;

**ANOVA**- Analysis of variance;

**BCA**- Bicinchoninic acid;

**BSA**- Bovine serum albumin;

**CCT**- "Coleção de Culturas Tropical" (Collection of tropical cell culture);

**HFBII**- Hydrophobin II;

**MALDI-TOF/TOF**- Matrix assisted laser desorption ionization-time of flight/time of flight;

**PDI**- Polydispersity index;

**RP-HPLC**- Reversed-phase high performance liquid chromatography;

**SDS-PAGE**- Sodium dodecyl sulphate-polyacrylamide gel electrophoresis;

**SEM**- Scanning electron microscopy;

$\gamma_0$- Surface tension of the bare interface;

$\gamma$- Surface tension;

$\Pi$- Surface pressure.

## 1. INTRODUCTION

Carrier systems stabilized by biopolymers have been broadly exploited in food technology for the incorporation of poorly water-soluble molecules (Araiza-Calahorra, Akhtar, & Sarkar, 2018; Dickinson, 2017; Fan, Yi, Zhang, Wen, & Zhao, 2017; Lam & Nickerson, 2013). Generally, biopolymers have exceptional intrinsic properties including the ability to form structured interfacial films (Dickinson, 2017), biofunctionality/biocompatibility (Sarparanta et al., 2012), biodegradability (Balakrishnan & Jayakrishnan, 2005), as well as potential for bioactivity (Khalesi et al., 2016). The interfacial property of these biopolymers has several purposes in food and pharmaceutical technology, such as the co-assembly with hydrophobic molecules (Akanbi et al., 2010; Israeli-Lev & Livney, 2014; Israeli-Lev et al., 2017; Valo et al., 2010) and the stabilization of emulsion systems (Dickinson, 2017; Fan, Yi, Zhang, Wen, & Zhao, 2017; Paukkonen, Ukkonen, Szilvay, Yliperttula, & Laaksonen, 2017).

Certain proteins are biopolymers that can be applied to stabilize emulsion systems due to their amphiphilic nature (Dickinson, 2017; Fan, Yi, Zhang, Wen, & Zhao, 2017). Hydrophobin II (HFBII) is a small protein (≈ 71 amino acids) produced by the filamentous fungus *Trichoderma reesei* (Askolin, Nakari-Setala, & Tenkanen, 2001; Kallio, Linder, & Rouvinen, 2007; Linder, 2009; Linder, Szilvay, Nakari-Setala, & Penttila, 2005). A globular $\beta$-barrel structure linked with a single $\alpha$-helix (≈ 7.2 kDa) forms the HFBII, which is stabilized by four disulfide bridges and characterized by its high-water solubility (Kallio, Linder, & Rouvinen, 2007; Linder, 2009; Linder, Szilvay, Nakari-Setala, & Penttila, 2005). Amino acids permanently exposed on the molecule surface provide its surfactant property serving for multiple purposes to the *T. reesei* spores (Kallio, Linder, & Rouvinen, 2007; Linder, 2009; Linder, Szilvay, Nakari-Setala, & Penttila, 2005; Sunde, Pham, & Kwan, 2017). Previous studies have shown the

capacity of hydrophobins to stabilize oil-in-water conventional emulsions using high-energy emulsification processes (Dimitrova et al., 2016; Guzmann, Eck, & Baus, 2013; Lumsdon, Green, & Stieglitz, 2005; Paukkonen, Ukkonen, Szilvay, Yliperttula, & Laaksonen, 2017). However, to the best of our knowledge, the use of HFBII to stabilize oil-in-water nanoemulsions produced by a low-energy emulsification process and the characterization of its interfacial properties have not yet been studied.

Oil-in-water nanoemulsion consists of nanoscale oil droplets dispersed into an aqueous medium and kinetically stabilized by surfactant molecules (Anton, Benoit, & Saulnier, 2008; McClements, 2012). The development of protein-stabilized nanoemulsions has gained attention with the use of bioactive lipids to form oily nutraceutical compartments (Fan, Yi, Zhang, Wen, & Zhao, 2017; Komaiko & McClements, 2015; McClements, Decker, Park, & Weiss, 2009). These molecules have a wide range of biological properties limited by their low solubility in water, which can be overcome by the exceptional ability of proteins to form viscoelastic films on droplet surfaces (Araiza-Calahorra, Akhtar, & Sarkar, 2018; Dickinson, 2017; McClements, Decker, Park, & Weiss, 2009). Copaiba is a natural oil found in trees of the genus *Copaifera* spp., whose studies have been performed due to its health-promoting properties. The sesquiterpenes and diterpenes present in this oleoresin promote biological properties, such as anti-inflammatory and antimicrobial activities, which could have potential in food applications (Alencar et al., 2015; Dias et al., 2014; McClements, Decker, Park, & Weiss, 2009).

The knowledge of formulation parameters is mandatory to improve the physical-chemical properties of protein-stabilized colloidal systems (Dickinson, 2015). Spontaneous emulsification processes represent non-aggressive mixing mechanisms largely applied to soft molecules (Anton, Benoit, & Saulnier, 2008; Bouchemal,

Briancon, Perrier, & Fessi, 2004; Komaiko & McClements, 2015). However, the production of nanoscale droplets by a low-energy process depends on the system composition to achieve an optimal droplet disruption (Bouchemal, Briancon, Perrier, & Fessi, 2004; Lee & McClements, 2010), which can be provided by a rational experimental design approach. In addition, the adsorption layer of proteins can be modified by the aqueous phase composition (e.g., ionic strength, pH), which directly affects the nanoemulsion system stability (Salis et al., 2011).

The aim of this study was to produce HFBII-stabilized nanoemulsions by a spontaneous emulsification process using copaiba oil as a bioactive lipid. To achieve this aim, HFBII protein was isolated from the wild-type *T. reesei* QM9414 and characterized. A factorial design approach was used to determine the optimal composition of the nanoemulsion system. In the last step, the effects of electrolytes on the physical-chemical properties of the optimal nanoemulsion system were analyzed.

## 2. MATERIALS AND METHODS

### 2.1. Materials

*T. reesei* strain QM9414 was acquired from the André Tosello foundation (CCT 2768, Campinas, SP, Brazil). Copaiba oil (*Copaifera langsdorffii*) was purchased from Flores e Ervas (São Paulo, Brazil) and characterized by Xavier-Júnior et al. (2017). Lactose monohydrated was acquired from Sigma Aldrich (St. Louis, USA). Acetonitrile and trifluoroacetic acid were obtained from J.T. Baker (Phillipsburg, USA). Acetone, sodium hydroxide (NaOH), hydrochloric acid (HCl) and phosphoric acid ($H_3PO_4$) were purchased from Vetec Química Fina (Rio de Janeiro, Brazil). All chemicals were of analytical or reagent grade and were used without further purification. Ultrapure water

191 was obtained from a water purification system (Q-POD®, Millipore, Germany) with
192 resistivity and total organic carbon of 18.2 MΩ.cm and 3 ppb at 25 °C, respectively.
193
194 **2.2. Fungal culture conditions**
195 *T. reesei* strain QM9414 was cultivated in an orbital shaking incubator (TE-420®,
196 Tecnal, Brazil) at 200 rpm and 25 °C, as described by Khalesi et al. (2013). HFBII was
197 produced into 500 mL flasks containing a liquid medium (120 mL) with lactose as
198 carbon source (Khalesi et al., 2013). The final pH of the liquid medium was adjusted to
199 4.5 with 10% $_{(v/v)}$ $H_3PO_4$. The growth kinetics of the *T. reesei* strain was manually
200 analyzed by nephelometry (HI 98703®, Hanna Instruments, Italy) using a mycelial
201 biomass-to-ultrapure water ratio of 1:10. Measurements were made during 7 days of
202 culture. Protein-rich supernatant was collected on the fourth day of culture by
203 centrifugation of the liquid medium (Gusto®, Fisherbrand, USA) at 8.000 *g* for 25 min.
204
205 **2.3. Purification and characterization of the HFBII**
206 The technique of protein extraction with $CO_2$ was used to obtain the HFBII-rich
207 fraction (Khalesi et al., 2013). HFBII was isolated by analytic RP-HPLC
208 (ÄKTApurifier®, Amersham Biosciences, Sweden) (15 RPC® column, 3 mL; GE
209 Healthcare, USA), with a 0-60% acetonitrile gradient elution containing 0.1%
210 trifluoroacetic acid at a flow rate of 2 mL.min$^{-1}$ and UV detection at 214 nm (Khalesi et
211 al., 2013). The organic solvent was removed by rotatory evaporator (RV 10® basic,
212 IKA, Germany) at 25 °C. The final pH of the protein solution was adjusted to 7.4 with 1
213 N NaOH. In all purification steps, a protein fraction was collected for quantification and
214 characterization analyses. The protein content was determined by the method of
215 bicinchoninic acid (BCA) with a protein assay kit (Pierce®, Thermo Scientific, USA) in

which bovine serum albumin (BSA) was used as standard (Araújo et al., 2016). The degree of purity of HFBII was evaluated by surface tension ($\gamma$) analysis (see Section *2.7.1.*) in which the same volume was collected from the purification fractions and diluted with ultrapure water (0.01 wt% culture supernatant, 0.008 wt% extraction ($CO_2$) and 0.002 wt% isolation (RP-HPLC)). The results were expressed numerically by the surface pressure ($\Pi$) ($\Pi = \gamma_0 - \gamma$).

### *2.3.1. Sodium dodecyl sulphate-polyacrylamide gel electrophoresis (SDS-PAGE)*

Protein fractions were subjected to SDS-PAGE (SE 600 Ruby®, Amersham Biosciences, Sweden), which was performed on a homogeneous 15% polyacrylamide gel (Araújo et al., 2016). The samples were prepared as described by Araújo et al. (2016). The molecular marker was used in the range of 6.5-200 kDa (SigmaMarker®, Sigma-Aldrich, USA), and protein bands were stained with silver (Laemmli, 1970).

### *2.3.2. Mass spectrometry*

The identification of intact protein was performed by MALDI-TOF-MS (Autoflex III®, Bruker Daltonik, Germany). Mass spectrum was obtained in the range of 2000-20000 Da and at frequency of 47 Hz. A protein standard (Bruker Daltonik, Bremen, Germany) was used as external calibration: insulin ($[M+H]^+$ 5734.51 m/z), cytochrome C ($[M+2H]^{2+}$ 6180.99 m/z), myoglobin ($[M+2H]^{2+}$ 8476.65 m/z), ubiquitin ($[M+H]^+$ 8565.76 m/z), cytochrome C ($[M+H]^+$ 12360.97 m/z) and myoglobin ($[M+H]^+$ 16952.30 m/z). The identification of peptides was performed by MALDI-TOF MS/MS at frequency of 100 Hz and in the range of 1000-8040 Da using BSA (Sigma-Aldrich, St. Louis, USA) as the internal mass calibrator. Acquisitions were performed in positive ion reflection mode. The ions were accelerated by 20 kV. The samples were prepared

241 according to Khalesi et al. (2016). Briefly, the sample (1 μL) was spotted onto a target
242 plate (MTP 384® ground steel, Bruker Daltonik, Germany) and mixed with the matrix
243 solution (1 μL). For peptide similarity search, the Fragment Ion Calculator® (Proteomics
244 Toolkit) was used to compare the observed fragment ions with the UniProt database of
245 the HFBII (ID P79073).
246
247 **2.4. Production of the nanoemulsion systems**
248 Oil-in-water nanoemulsions were produced by a spontaneous emulsification
249 process (Bouchemal, Briancon, Perrier, & Fessi, 2004; Yu et al., 1993). The aqueous
250 phase was composed of HFBII (0.005, 0.0175, and 0.030 wt%) in ultrapure water, while
251 the organic phase was composed of copaiba oil (0.02, 0.06, and 0.10 wt%) in acetone.
252 Glass tubes containing the aqueous phase were sonicated into an ultrasonic bath (USC-
253 1800A®, UNIQUE, Brazil) for 1 min to disperse protein aggregates and to remove small
254 bubbles. Then, the organic phase (100 μL) was slowly injected into the aqueous phase
255 (1 mL) under magnetic stirring (C-MAG HS 7®, IKA, USA) at 750 rpm and at 25 °C.
256 To completely evaporate the acetone, the samples were heated (ETS D5®, IKA, USA) at
257 50 °C for 60 min under moderate magnetic stirring. After 24 h, the physical-chemical
258 analyses of the nanoemulsion systems were performed.
259
260 **2.5. Experimental factorial design**
261 A $2^3$-full factorial design approach with three central points was used to optimize
262 the production of a nanoemulsion system with small values of droplet size and PDI, as
263 well as high absolute values of zeta potential. A total of 11 experiments were prepared
264 as described in Section 2.4. using the contents of HFBII (0.005, 0.0175, and 0.030
265 wt%), copaiba oil (0.02, 0.06, and 0.10 wt%) and the organic-to-aqueous phase ratio

(10, 30, and 50% $_{(v/v)}$) as independent variables. The protein contents were chosen based on the literature data (Basheva et al., 2011a; Dimitrova et al., 2016). The factors droplet size, polydispersity index (PDI) and zeta potential were selected as dependent variables. Statistical data analyses were performed using the Statistica® software (Version 7.0, StatSoft Inc., USA) to validate the factorial design. Response surface plots were generated to visualize the simultaneous effect of each variable on each response parameter.

## 2.6. Influence of ionic strength and pH on the HFBII-stabilized nanoemulsion

The effects of electrolytes on physical-chemical properties of the optimal nanoemulsion system, selected based on the experimental Section 2.5., were analyzed for 7 days. In the first set of experiments, the ionic strength in the aqueous phase was adjusted to 25, 250 or 500 mM NaCl, and the pH was maintained at 7.4. In the next experiments, the pH of the aqueous phase was adjusted to 2, 6, 7.4 or 10 (MPT-2®, Malvern, UK), using a solution of 1 N HCl or 1 N NaOH, and the ionic strength was maintained at the lowest value (<25 mM NaCl). The aqueous phase composition was modified before the production of the nanoemulsion system. Physical-chemical characterizations were performed to establish a correlation between the aqueous phase composition and the nanoemulsion system stability.

## 2.7. Physical-chemical analyses

### *2.7.1. Pendant drop measurements*

The dynamic surface tension ($\gamma$) was obtained by measuring the drop relaxation as a function of time, using the Contact-Angle-Drop-Shape-Analysis System 100® (Krüss, Germany) with the DSA3® software. Drops were formed by a motor-driven

291 microsyringe using a stainless-steel needle. Measurements were performed at the time
292 interval of 5 s by analyzing the drop-shape with a high-resolution camera (25 pictures
293 per second). The samples containing 0.002 wt% HFBII in ultrapure water were
294 evaluated after adjusting the ionic strength and pH of the aqueous phase.

295

296 *2.7.2. Dynamic light scattering*

297 The hydrodynamic diameter and size distribution of the nanoemulsion systems
298 were measured by Zetasizer Nano-ZS® (Malvern, UK). The samples were diluted to a
299 concentration of about 0.0025 wt% with ultrapure water, and loaded into a polystyrene
300 cuvette (DTS0012®, Malvern, UK). The measurements were performed at 25 °C using
301 an angle of detection of 173º, a refractive index of 1.33 for the dispersion medium and
302 1.45 for the nanoemulsion system, and a viscosity of the dispersion medium of 0.89.

303

304 *2.7.3. Zeta potential*

305 The zeta potential of the nanoemulsion systems was measured (Zetasizer Nano-
306 ZS®, Malvern, UK) using the samples and measurement parameters previously
307 described (see Section *2.7.2.*). The dielectric constant of the dispersion medium was
308 78.5. A folded capillary cell (DTS1070®, Malvern, UK) was used for the zeta potential
309 analysis.

310

311 *2.7.4. Atomic force microscopy (AFM)*

312 AFM micrographs were obtained on the SPM-9700® (Shimadzu, Japan) operating
313 in the tapping mode at room temperature. The samples containing 0.002 wt% HFBII in
314 ultrapure water were spread on mica leaf and exposed for 48 h at room temperature to
315 dry. The silicon cantilevers (Pointprobe®, NanoWorld AG, Switzerland) with a spring

316 constant in the range of 21-78 N/m were used to obtain the images. The drive frequency
317 was set at 320 kHz, and the scan rate was 1.0 Hz. For each sample, a scan area of 5 µm
318 x 5 µm was analyzed.
319
320 *2.7.5. Scanning electron microscopy (SEM)*
321 The droplet morphologies of the HFBII-stabilized nanoemulsion were evaluated by
322 SEM EVO LS15® (Carl Zeiss, Germany) with an acceleration voltage of 10 kV. The
323 samples (10 µL) were placed onto a glass cover, dried at room temperature and sputter-
324 coated with gold in an ion-sputtering apparatus (Q150T ES®, Quorum Technologies,
325 UK) to avoid charging under the electron beam and to enhance the image contrast.
326
327 **2.8. Statistical analyses**
328 Most experiments were carried out in duplicate and the results expressed as the
329 mean ± S.D. The means of two groups were compared using non-paired Student's t-
330 tests. When comparing multiple groups, one-way analysis of variance (ANOVA) was
331 applied with the Tukey multiple comparisons. The statistical data were considered
332 significant at $p$-value <0.05. The software GraphPad Prism® (Version 5.0, GraphPad
333 Software Inc., USA) and the Statistica® (Version 7.0, StatSoft Inc., USA) were used to
334 perform the statistical analyses of the data.
335
336 **3. RESULTS AND DISCUSSION**
337 **3.1. Purification and characterization of the HFBII**
338 The analysis of growth kinetics by nephelometry provided a typical microbial
339 growth curve (Figure 1S) allowing the identification of the *T. reesei* at the stationary
340 phase. This step corresponds to the microbial sporulation phase in which the HFBII

production occurs (Khalesi et al., 2014). Thus, the fourth day of culture of the *T. reesei* was selected to obtain the HFBII-rich supernatant for the extraction step by $CO_2$. The isolated fractions by RP-HPLC were eluted with 46% $_{(v/v)}$ acetonitrile. The technique of SDS-PAGE identified bands of an approximate molar mass of 7 kDa, and indicated that the purification steps of extraction with $CO_2$ (Figure 1 (A) – lane 2) and isolation by RP-HPLC (Figure 1 (A) – lane 3) were able to remove other contaminant proteins.

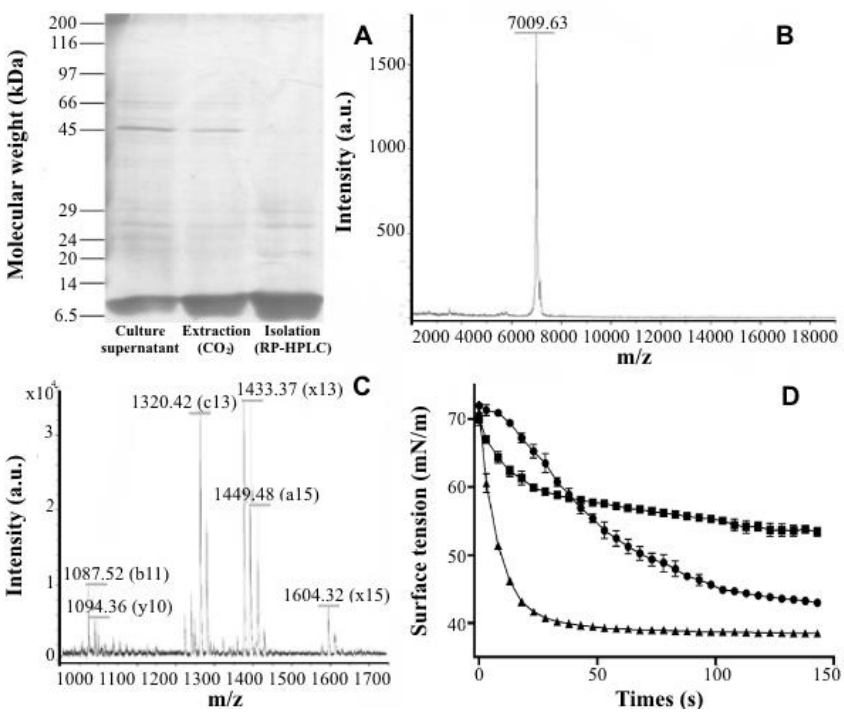


**Figure 1**- Purification of HFBII. Silver stained SDS-PAGE of the HFBII purification steps (A). Mass spectrum of the intact HFBII obtained from MALDI-TOF/TOF (B). Mass spectrum of the ion fragments of HFBII (C). Dynamic surface tension ($\gamma$) of protein fractions from the purification steps (● 0.01 wt% culture supernatant, ▲ 0.008 wt% extraction ($CO_2$) and ■ 0.002 wt% isolation (RP-HPLC)) (D).

356 The intact protein analyzed by MALDI-TOF/TOF confirmed the presence of a
357 single peak at molar mass of 7009.6 Da (Figure 1 (B)). The peptide analysis provided
358 details concerning the specific ion fragments in the range of 1000-1700 Da (Figure 1
359 (C)). In addition, a series of 6 ion fragments can be attributed to the amino acid
360 sequences corresponding to the subsets of peptides calculated from the HFBII database
361 (Table 1S). In this sense, the analyses of the intact protein and individual peptides not
362 only confirmed the HFBII identity, but also corroborated the previous study in which
363 HFBII was obtained with a molar mass of 7042.0 Da (Khalesi et al., 2013).
364 The relaxation of the air-water surface tension ($\gamma$) was measured by adsorption of
365 molecules as a function of time in order to determine the HFBII surface activity (Figure 1
366 (D)). The adsorption kinetics of proteins at fluid interfaces is subdivided into four stages: (1)
367 diffusion, (2) adsorption, (3) conformational reorganization and (4) consolidation of the
368 protein film (Dickinson, 2011). Culture supernatant showed a first stage of short lag time to
369 reduce the surface tension ($\gamma$). As the drop surface becomes saturated, a smooth reduction of
370 surface tension ($\gamma$) occurs until reach a partial steady-state condition, which characterizes a
371 diffusion-limited stage regulated by a set of contaminant proteins (Dickinson, 2011).
372 An abrupt decrease in surface tension ($\gamma$) was verified in the experimental curves of the
373 extracted and isolated fractions, which indicates a rapid diffusion rate and surface adsorption
374 of the protein molecules after the drop formation. The latter events were confirmed by the
375 lack of a first stage and by the short time of the second stage (≈3-28 s) to reach a partial
376 steady-state condition, which suggests a high degree of purity. The extraction with $CO_2$
377 presented the greatest decrease in surface tension ($\gamma$). These results are consistent with
378 Khalesi et al. (2013) who described the foam fractionation with $CO_2$ as an effective
379 technique to concentrate surfactant proteins. The time-dependent adsorption of the isolated
380 fraction (≈3-28 s) was shorter than the culture supernatant (≈13-93 s), although the former

was the lowest concentrated sample. Taking together all the results of dynamic surface tension ($\gamma$), it can be concluded that the surface tension ($\gamma$) decreases according to the concentration and purity of the protein solution.

As seen in Table 1, the surface activity of HFBII was improved after the purification steps. The isolated HFBII presented a specific surface activity of 46.5 $mN.m^{-1}.\mu g^{-1}$, indicating an overall purification of about 3.2-fold. The removal of contaminant proteins with lower surface activity explains the decrease in total activity after the isolation step, while the specific activity could be increased (Liang, Hsieh, & Wang, 2012). Thus, the combination of the extraction and isolation steps was an effective method for the high degree of purification of HFBII.

**Table 1-** Purification steps of the HFBII from the culture of the *T. reesei* QM9414.

| Steps | Total protein (mg) | Protein analyzed (µg) | Total activity ($mN.m^{-1}$) | Specific activity ($mN.m^{-1}.\mu g^{-1}$) | Purification fold |
|---|---|---|---|---|---|
| **Culture supernatant** | 750.0 | 2.0 | 29.0 | 14.5 | 1.0 |
| **Extraction ($CO_2$)** | 426.0 | 1.6 | 33.5 | 21.0 | 1.4 |
| **Isolation (RP-HPLC)** | 4.5 | 0.4 | 18.6 | 46.5 | 3.2 |

### 3.2. Production of the nanoemulsion systems

The process to optimize the production of nanoscale droplets depends on the experimental variables as the homogenization conditions (e.g., equipment, duration), the system composition (e.g., organic phase, aqueous phase), and the nature/concentration of the emulsifier (e.g., adsorption kinetics, interfacial tension) (Lee & McClements,

399 2010). The experimental design was applied to minimize the experiments required to
400 produce a nanoemulsion system with small values of droplet size and PDI, as well as
401 high absolute values of zeta potential, which would be predictive of higher stability.

402 As presented in Table 2, the dependent variables ranged from 149.6 to 343.1 nm
403 (droplet size), 0.153 to 0.402 (PDI) and -28.0 to -44.2 mV (zeta potential). The
404 significant effects ($p$-value <0.05) of the independent variables (HFBII and copaiba oil
405 concentrations, and organic-to-aqueous phase ratio) on the dependent variables were
406 analyzed by the Pareto chart and the response surface graphics.

407

408 **Table 2-** Independent variables chosen to produce nanoemulsion systems with low
409 values of droplet size and PDI, as well as high absolute values of zeta potential.

| Samples | Independent variables | | | Dependent variables | | |
|---|---|---|---|---|---|---|
| | **HFBII (wt%)** | **Copaiba oil (wt%)** | **Organic-to-aqueous phase ratio (v/v)** | **Droplet size ± S.D. (nm)** | **PDI ± S.D.** | **Zeta potential ± S.D. (mV)** |
| **N1** | 0.030 | 0.10 | 50 | 236.0 ± 2.7 | 0.192 ± 0.008 | -31.6 ± 1.9 |
| **N2** | 0.030 | 0.02 | 50 | 221.1 ± 15.1 | 0.252 ± 0.015 | -36.7 ± 1.6 |
| **N3** | 0.005 | 0.10 | 10 | 343.1 ± 6.3 | 0.402 ± 0.004 | -44.0 ± 3.4 |
| **N4** | 0.030 | 0.02 | 10 | 214.5 ± 1.8 | 0.190 ± 0.038 | -34.3 ± 0.4 |
| **N5** | 0.005 | 0.10 | 50 | 233.8 ± 4.4 | 0.164 ± 0.013 | -43.4 ± 1.5 |
| **N6** | 0.005 | 0.02 | 50 | 149.6 ± 4.3 | 0.239 ± 0.013 | -28.0 ± 1.4 |
| **N7** | 0.030 | 0.10 | 10 | 254.1 ± 1.8 | 0.242 ± 0.004 | -40.8 ± 0.7 |
| **N8** | 0.005 | 0.02 | 10 | 154.2 ± 2.6 | 0.153 ± 0.025 | -29.1 ± 3.2 |
| **N9** | 0.0175 | 0.06 | 30 | 265.3 ± 4.8 | 0.223 ± 0.028 | -39.3 ± 3.4 |
| **N10** | 0.0175 | 0.06 | 30 | 261.8 ± 1.0 | 0.231 ± 0.022 | -44.2 ± 2.4 |
| **N11** | 0.0175 | 0.06 | 30 | 240.7 ± 2.2 | 0.210 ± 0.008 | -42.1 ± 0.8 |

410

411 The factor copaiba oil concentration, and the association between the factors HFBII
412 and copaiba oil concentrations promoted significant effects ($R^2$ = 0.9866 by ANOVA
413 analysis) on the dependent variable, droplet size (Figure 2S). Also, all the evaluated
414 factors and their associations, except for the factor HFBII, were statistically significant
415 ($R^2$ = 0.9918 by ANOVA analysis) on the dependent variable, PDI.

416 The response surface graphic (Figure 2 (A)) revealed that low oil concentration was
417 the main factor to achieve the small values of droplet size, which can be directly
418 correlated to the emulsification process. In general, the spontaneous emulsification
419 involves the disruption of droplets by diffusing a water-miscible solvent from the
420 organic phase into the aqueous phase (Bouchemal, Briancon, Perrier, & Fessi, 2004; Yu
421 et al., 1993). Thus, the disruption was improved by the greater diffusion of the acetone
422 through the oil-water interface at low oil content, which formed droplets with large
423 surface area (Lee & McClements, 2010; McClements, 2012).

424 In addition, Tcholakova et al. (2003) described the occurrence of fusion of
425 neighboring droplets at low protein concentrations until reaching a molecule adsorption
426 threshold to stabilize the interface. At low oil content, the HFBII hydrophobic attraction
427 to the interface may be favored by the formation of oil droplets with large surface area, after
428 the diffusion of acetone, promoting the rapid structuration of adsorption layers. The
429 exceptionality of the HFBII structure arises from the exposed hydrophobic region,
430 which permits a rapid adsorption on oily surfaces to form layers of high mechanical
431 strength even at low protein concentrations ($10^{-3}$ wt%) (Basheva et al., 2011b;
432 Dimitrova et al., 2016; Kallio, Linder, & Rouvinen, 2007; Radulova et al., 2012).

433

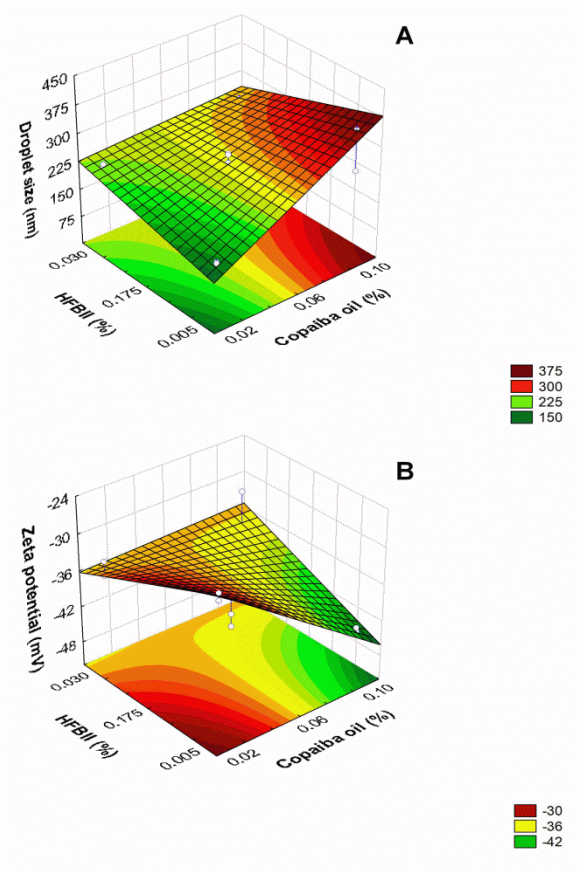


434

435 **Figure 2**- Response surface diagrams of the factors HFBII (%) and copaiba oil (%)

436 concentrations on droplet size (A) and zeta potential (B).

437

438 The association between the factors HFBII and organic-to-aqueous phase ratio was

439 significant for the increase on the values of PDI (Figure 2S). High acetone concentration

440 probably hampered the adsorption of the HFBII on the droplet surfaces by interaction

441 with the hydrophobic region of the protein (Kisko, Szilvay, Vainio, Linder, & Serimaa,

442 2008). Therefore, low acetone content was an important factor to achieve a narrow

443 droplet size distribution, as well as to support the environmental and biocompatibility

444 issues attributed to the nanoemulsion system.

445 Only the factor copaiba oil concentration promoted a significant effect ($R^2$ = 0.9667

446 by ANOVA analysis) on the dependent variable, zeta potential (Figure 2 (B)). This

447 result may be due to the adsorption of the carboxylate anions formed by the

sesquiterpenes and the diterpenes present in this oleoresin. During the acetone evaporation step, these volatile carboxylate anions may be trapped on the droplet surfaces, which led to the increase in negative charge (Dias et al., 2014).

According to the results obtained using the experimental design, the nanoemulsion system (N8) achieved small values of droplet size (154.2 ± 2.6 nm) and PDI (0.153 ± 0.025), as well as a high absolute value of zeta potential (-29.1 ± 3.2 mV) with 0.005 wt% HFBII, 0.02 wt% copaiba oil and 10% $_{(v/v)}$ organic-to-aqueous phase ratio. Therefore, the N8 formulation was selected as the optimal HFBII-stabilized nanoemulsion.

### 3.3. Influence of ionic strength and pH on the HFBII-stabilized nanoemulsion

Changes in aqueous phase composition by addition of electrolytes (e.g., acids, bases and salts) directly affect the function-structure of biopolymers at interfaces (Lam & Nickerson, 2013; Tcholakova, Denkov, Sidzhakova, Ivanov, & Campbell, 2005). In this set of experiments, the optimal HFBII-stabilized nanoemulsion (N8) was prepared with modifications in the ionic strength and pH of the aqueous phase.

#### *3.3.1. Influence of ionic strength*

The effect of ionic strength on physical-chemical properties of the nanoemulsion system was determined at constant pH of 7.4 (Figure 3 (A) and Figure 3 (B)). The samples with low salt content (≤25 mM NaCl) were stable during 7 days with small droplet sizes (<250 nm) (*p*-value >0.05) and moderate absolute value of zeta potential (<-25 mV). However, the increase in salt content in the aqueous phase (>25 mM NaCl) had an appreciable impact on the increase in droplet size (*p*-value <0.05). Furthermore,

a decrease of -33 to -22 mV was observed in the absolute value of the zeta potential (Figure 3 (B)).

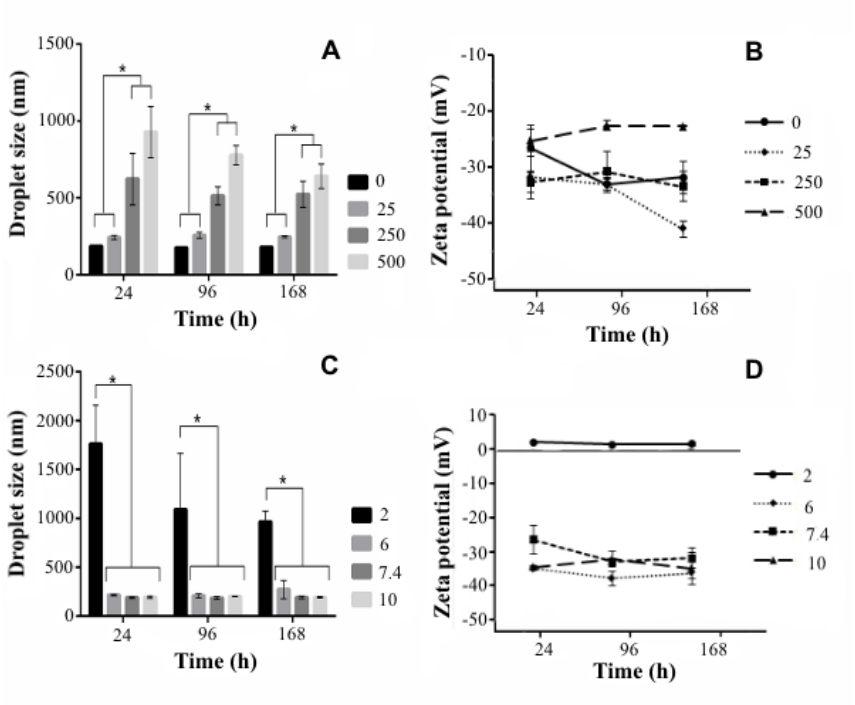


**Figure 3**- Droplet size (A) and (C) and zeta potential (B) and (D) of the HFBII-stabilized nanoemulsion containing copaiba oil as a function of the ionic strength (A) and (B) – 0, 25, 250, 500 – and the pH (C) and (D) – 2, 6, 7.4, 10 – during 7 days.

The system stability was governed by the electric potential of the HFBII film, which forms a repulsive barrier to prevent the flocculation of oil droplets (Tcholakova, Denkov, Sidzhakova, Ivanov, & Campbell, 2005). At low salt content (≤25 mM NaCl), the electric double layer is sufficiently strong to overcome the attractive forces between the droplet surfaces. However, the exposure to high concentrations of $Na^+$ decreased the charge density and, probably, promoted the desolvation of the HFBII molecules, which favor the occurrence of hydrophobic interactions and protein aggregation (Basheva et

al., 2011b; Peng, Liu, Zhao, & Zhou, 2014). Hence, the droplet flocculation probably occurred by the disruption of the electrostatic repulsion and the mechanical protection, previously, provided by the monolayer of HFBII (Basheva et al., 2011a; Tcholakova, Denkov, Sidzhakova, Ivanov, & Campbell, 2005).

### *3.3.2. Influence of pH*

Aiming to study the effect of pH on physical-chemical properties of the nanoemulsion system, the ionic strength of the aqueous phase was maintained at the lowest value (<25 mM NaCl). Large droplet size ($d \approx 1270$ nm) ($p$-value <0.05) and zeta potential close to the neutrality were obtained to the samples at acid aqueous phase (Figure 3 (C) and 3 Figure (D)). Meanwhile, the samples formulated at pH 6, 7.4 and 10 showed small droplet sizes (<300 nm) ($p$-value >0.05) and moderate absolute value of zeta potential (<-25 mV) during 7 days.

The nanoemulsion system stability at high pH values can be attributed to the electric potential of the droplet surfaces (Salis et al., 2011). In addition, the low charge density (zeta potential ≈ 1.5 mV) supports the hypothesis of the proximity to the HFBII isoelectric point (≈ pH 3.5) at pH 2 (Burke, Cox, Petkov, & Murray, 2014). Hence, the droplet-droplet electrostatic repulsion is hampered at the pH around the isoelectric point when compared to the other pH conditions (pH 6, 7.4, 10), which reduces repulsive forces (Basheva et al., 2011b). Furthermore, the lower nanoemulsion system stability in the acidic medium is associated with the unfolding of the HFBII secondary structure (Kisko, Szilvay, Vainio, Linder, & Serimaa, 2008). Changes in protein structure can disrupt the mechanical protection attributed to the compact adsorption layer of HFBII on the oil-water interface (Radulova et al., 2012).

### 3.4. Microstructural properties of the HFBII film

The production of stable oil dispersions covered by surfactant proteins requires a short time of adsorption, optimal surface coverage and electrical charge (Lam & Nickerson, 2013). In this study, the surfactant function and the adsorption structure of the HFBII were analyzed in different salt contents (0 or 25 mM NaCl) and pH values (6 or 7.4) selected according to the previous study.

A rapid decrease in surface tension ($\gamma$) was observed for all samples as the protein adsorbs on the air-water interface ($p$-value >0.05) (Figure 4 (A) – insert). Therefore, the adsorption kinetics and surface activity of the HFBII were maintained in the electrolyte concentrations used. In this sense, the surfactant function of the HFBII should allow the development of a HFBII-stabilized nanoemulsion at low salt content and pH values close to the neutrality.

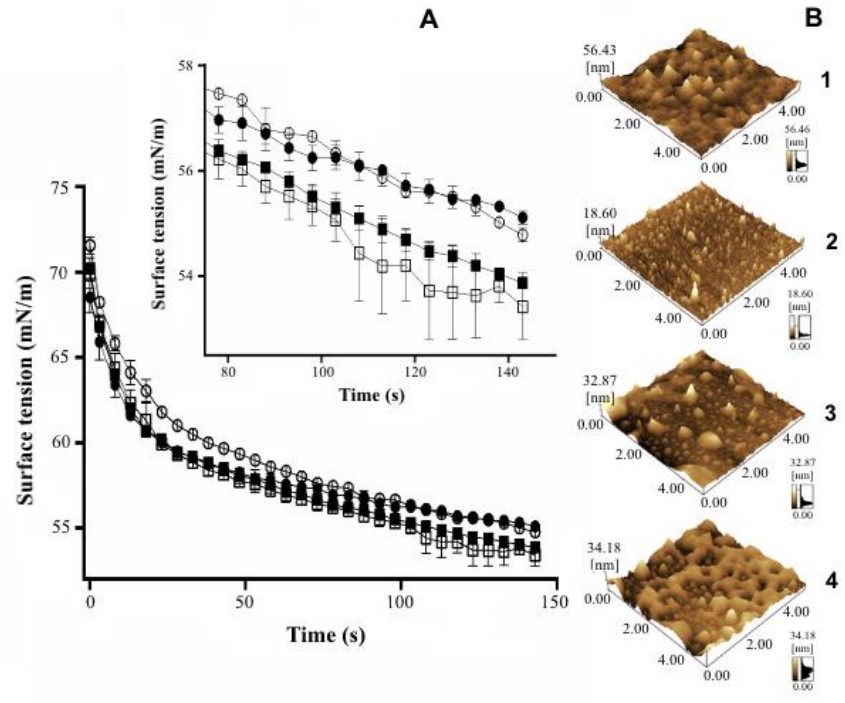


**Figure 4**- Influence of the electrolyte contents on the function-structure of the HFBII film. Dynamic surface tension ($\gamma$) of aqueous solutions containing 0.002

wt% HFBII (○ pH 6, □ pH 7.4, ● pH 6 + 25 mM NaCl and ■ pH 7.4 + 25 mM NaCl) (A). AFM micrographs of the adsorption layer of HFBII (0.002 wt%) onto mica under pH 6 (1), pH 7.4 (2), pH 6 + 25 mM NaCl (3) and pH 7.4 + 25 mM NaCl (4) (B).

The protein was morphologically characterized by AFM as clusters of conical shape (Figure 4 (B.1-4)). The thicker regions of protein aggregates were identified as bright spots, whereas the dark spots correspond to voids in the protein film. The protein dispersion at pH 6 was remarked by empty areas and regions of HFBII aggregates resembling high plateaus (Figure 4 (B.1)) in which the height of protein clusters ranged from 24 to 57 nm. At pH 7.4 (Figure 4 (B.2)), the mica surface was covered by a monolayer of HFBII with relatively small empty areas and height of protein clusters ranging from about 3 to 19 nm. The addition of 25 mM NaCl promoted considerable changes in the surface topography characterized by large empty areas and inhomogeneous dispersion of HFBII (Figure 4 (B.3) and Figure 4 (B.4)).

Droplet micrographs by SEM of the HFBII-stabilized nanoemulsion showed elongated and spherical morphologies at pH 6 and 7.4, respectively, with size around 200-400 nm (Figure 5 (A) and Figure 5 (B)). The addition of salt (25 mM NaCl) hampered the visualization of nanoscale droplets and led to the formation of structures with irregular shapes and large size of about 3 μm, which may be salt crystals (Figure 5 (C) and Figure 5 (D)). Thus, the AFM results were corroborated by the SEM micrographs.

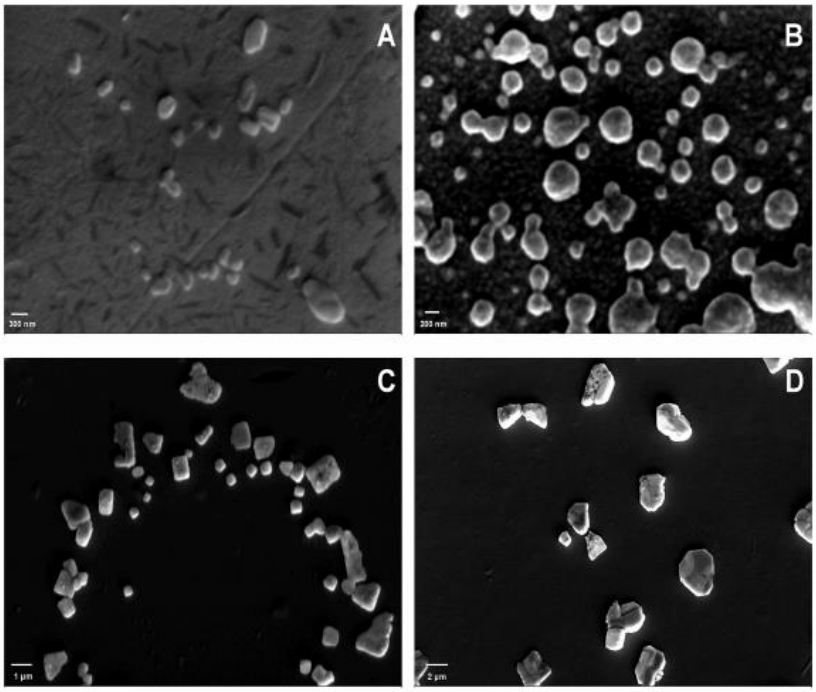


**Figure 5**- Droplet micrographs by SEM of the HFBII-stabilized nanoemulsion under pH 6 (A), pH 7.4 (B), pH 6 + 25 mM NaCl (C) and pH 7.4 + 25 mM NaCl (D).

The formation of a HFBII film on the oil-water interface involves limiting stages of oligomers dissociation and monomers/amphiphilic dimers diffusion by the displacement of their hydrophobic regions from the aqueous medium (Kallio, Linder, & Rouvinen, 2007). A second stage of short-range hydrophobic attraction promotes the adsorption of HFBII on the surface of oil droplets (Figure 6) (Cheung, 2012; Dickinson, 2011). The exposure of the HFBII to salt and acidic medium lowers the electrostatic barrier and increases the protein aggregates, which should not form a uniform layer structure (Basheva et al., 2011b). However, the HFBII film on the oil-water interface may consist of an interaction of monomers with thicker domains and empty regions (Figure 6). Therefore, the increase in the aggregate state of HFBII probably disrupted the oil droplet coverage promoting the instability of the nanoemulsion system (Lam & Nickerson, 2013).

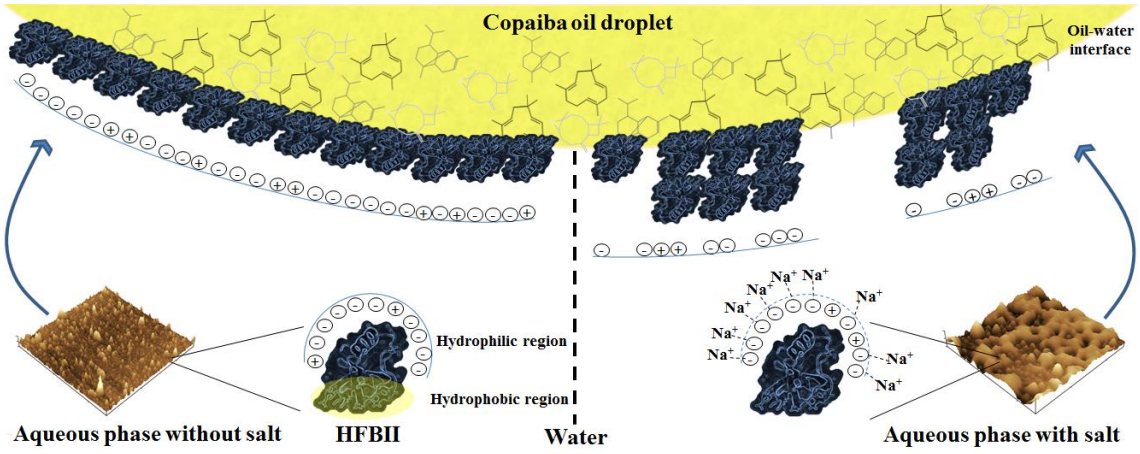


**Figure 6**- Overall scheme of the influence of the electrolytes on the formation of the HFBII film on the oil-water interface.

## 4. CONCLUSION

The present study demonstrated the feasibility of producing HFBII-stabilized nanoemulsions by a low-energy emulsification process. The HFBII protein was effectively isolated by the combination of two purification steps achieving an overall purification of about 3.2-fold. According to the experimental design approach, the optimal formulation was achieved with 0.005 wt% HFBII, 0.02 wt% copaiba oil and 10% $_{(v/v)}$ organic-to-aqueous phase ratio. The low copaiba oil concentration improved the spontaneous emulsification process to form nanoscale droplets, which probably favored the structuration of the adsorption layer of HFBII on the oil-water interface. HFBII-stabilized nanoemulsion was stable at low salt content (≤25 mM) and pH values close to the neutrality. In such conditions, the electric potential of the HFBII film was sufficiently strong to prevent the flocculation of the oil droplets. However, the aggregation behavior of the HFBII film exposed to high salt contents (≥25 mM NaCl) and acidic medium probably disrupted the protein coverage of oil droplets, as well as the nanoemulsion system stability. All these findings indicate the promising use of the

589 HFBII as a biopolymer to stabilize nanoemulsion systems to be used for the delivery of
590 bioactive lipids. Further studies should be performed to evaluate the stability of the
591 HFBII-stabilized nanoemulsion and the nutraceutical potential of its copaiba oil
592 droplets.
593
594 **Acknowledgements**

595 The authors are grateful to Dr. Gorete Ribeiro (UFRN, Brazil) for providing the
596 fungal strain. We also thank Dr. Elizabeth Santos (UFRN, Brazil) and Dr. Francisco
597 Canindé (UFRN, Brazil) for the technical assistance. Finally, the authors thank M.S.
598 Igor Zumba (UFRN, Brazil) and M.S. Rafael Padilha (UFPE, Brazil) for AFM and SEM
599 analyses, respectively. This study was supported by CNPq and CAPES.
600

601 **References**

602 Akanbi, H. J. M., Post, E., Meter-Arkema, A., Rink, R., Robillard, G. T., Wang, X.,
603 Wosten, H. A., & Scholtmeijer, K. (2010). Use of hydrophobins in formulation
604 of water insoluble drugs for oral administration. *Colloids Surf. B, 75*, 526-531.
605 Alencar, E. N., Xavier-Júnior, F. H., Morais, A. R. V., Dantas, T. R. F., Dantas-Santos,
606 N., Verissimo, L. M., Rehder, V. L. G., Chaves, G. M., Oliveira, A. G., & Egito,
607 E. S. T. (2015). Chemical characterization and antimicrobial activity evaluation
608 of natural oil nanostructured emulsions. *J. Nanosci. Nanotechnol., 15*, 880-888.
609 Anton, N., Benoit, J. P., & Saulnier, P. (2008). Design and production of nanoparticles
610 formulated from nano-emulsion templates-A review. *J. Control. Release, 128*,
611 185-199.

612 Araiza-Calahorra, A., Akhtar, M., & Sarkar, A. (2018). Recent advances in emulsion-
613 based delivery approaches for curcumin: From encapsulation to bioaccessibility.
614 *Trends Food Sci. Technol., 71*, 155-169.
615 Araújo, N. K., Pagnoncelli, M. G., Pimentel, V. C., Xavier, M. L., Padilha, C. E.,
616 Macedo, G. R., & Santos, E. S. (2016). Single-step purification of chitosanases
617 from *Bacillus cereus* using expanded bed chromatography. *Int. J. Biol.*
618 *Macromol., 82*, 291-298.
619 Askolin, S., Nakari-Setala, T., & Tenkanen, M. (2001). Overproduction, purification,
620 and characterization of the *Trichoderma reesei* hydrophobin HFBI. *Appl.*
621 *Microbiol. Biotechnol., 57*, 124-130.
622 Balakrishnan, B., & Jayakrishnan, A. (2005). Self-cross-linking biopolymers as
623 injectable *in situ* forming biodegradable scaffolds. *Biomater., 26*, 3941-3951.
624 Basheva, E. S., Kralchevsky, P. A., Christov, N. C., Danov, K. D., Stoyanov, S. D.,
625 Blijdenstein, T. B., Kim, H. J., Pelan, E. G., & Lips, A. (2011a). Unique
626 properties of bubbles and foam films stabilized by HFBII hydrophobin.
627 *Langmuir, 27*, 2382-2392.
628 Basheva, E. S., Kralchevsky, P. A., Danov, K. D., Stoyanov, S. D., Blijdenstein, T. B.,
629 Pelan, E. G., & Lips, A. (2011b). Self-assembled bilayers from the protein
630 HFBII hydrophobin: Nature of the adhesion energy. *Langmuir, 27*, 4481-4488.
631 Bouchemal, K., Briancon, S., Perrier, E., & Fessi, H. (2004). Nano-emulsion
632 formulation using spontaneous emulsification: Solvent, oil and surfactant
633 optimisation. *Int. J. Pharm., 280*, 241-251.
634 Burke, J., Cox, A., Petkov, J., & Murray, B. S. (2014). Interfacial rheology and stability
635 of air bubbles stabilized by mixtures of hydrophobin and *β*-casein. *Food*
636 *Hydrocoll., 34*, 119-127.

637 Cheung, D. L. (2012). Molecular simulation of hydrophobin adsorption at an oil-water
638 interface. *Langmuir, 28*, 8730-8736.
639 Dias, D. O., Colombo, M., Kelmann, R. G., Kaiser, S., Lucca, L. G., Teixeira, H. F.,
640 Limberger, R. P., Veiga, V. F., & Koester, L. S. (2014). Optimization of copaiba
641 oil-based nanoemulsions obtained by different preparation methods. *Ind. Crop.*
642 *Prod., 59*, 154-162.
643 Dickinson, E. (2011). Mixed biopolymers at interfaces: Competitive adsorption and
644 multilayer structures. *Food Hydrocoll., 25*, 1966-1983.
645 Dickinson, E. (2015). Colloids in food: Ingredients, structure, and stability. *Annu. Rev.*
646 *Food Sci. Technol., 6*, 211-233.
647 Dickinson, E. (2017). Biopolymer-based particles as stabilizing agents for emulsions
648 and foams. *Food Hydrocoll., 68*, 219-231.
649 Dimitrova, L. M., Boneva, M. P., Danov, K. D., Kralchevsky, P. A., Basheva, E. S.,
650 Marinova, K. G., Petkov, J. T., & Stoyanov, S. D. (2016). Limited coalescence
651 and Ostwald ripening in emulsions stabilized by hydrophobin HFBII and milk
652 proteins. *Colloids Surf. A, 509*, 521-538.
653 Fan, Y., Yi, J., Zhang, Y., Wen, Z., & Zhao, L. (2017). Physicochemical stability and
654 *in vitro* bioaccessibility of *β*-carotene nanoemulsions stabilized with whey
655 protein-dextran conjugates. *Food Hydrocoll., 63*, 256-264.
656 Guzmann, M., Eck, P., & Baus. (2013). Use of hydrophobin as a phase stabilizer. In
657 (Vol. US 8,535,535 B2, pp. 37). United States BASF SE.
658 Israeli-Lev, G., & Livney, Y. D. (2014). Self-assembly of hydrophobin and its co-
659 assembly with hydrophobic nutraceuticals in aqueous solutions: Towards
660 application as delivery systems. *Food Hydrocoll., 35*, 28-35.

Israeli-Lev, G., Pitchkhadze, M., Nevo, S., Fahoum, L., Meyron-Holtz, E., & Livney, Y. D. (2017). Harnessing proteins to control crystal size and morphology, for improved delivery performance of hydrophobic bioactives, using genistein as a model. *Food Hydrocoll., 63*, 97-107.

Kallio, J. M., Linder, M. B., & Rouvinen, J. (2007). Crystal structures of hydrophobin HFBII in the presence of detergent implicate the formation of fibrils and monolayer films. *J. Biol. Chem., 282*, 28733-28739.

Khalesi, M., Jahanbani, R., Riveros-Galan, D., Sheikh-Hassani, V., Sheikh-Zeinoddin, M., Sahihi, M., Winterburn, J., Derdelinckx, G., & Moosavi-Movahedi, A. A. (2016). Antioxidant activity and ACE-inhibitory of class II hydrophobin from wild strain *Trichoderma reesei*. *Int. J. Biol. Macromol., 91*, 174-179.

Khalesi, M., Venken, T., Deckers, S., Winterburn, J., Shokribousjein, Z., Gebruers, K., Verachtert, H., Delcour, J., Martin, P., & Derdelinckx, G. (2013). A novel method for hydrophobin extraction using $CO_2$ foam fractionation system. *Ind. Crop. Prod., 43*, 372-377.

Khalesi, M., Zune, Q., Telek, S., Riveros-Galan, D., Verachtert, H., Toye, D., Gebruers, K., Derdelinckx, G., & Delvigne, F. (2014). Fungal biofilm reactor improves the productivity of hydrophobin HFBII. *Biochem. Eng. J., 88*, 171-178.

Kisko, K., Szilvay, G. R., Vainio, U., Linder, M. B., & Serimaa, R. (2008). Interactions of hydrophobin proteins in solution studied by small-angle x-ray scattering. *Biophys. J., 94*, 198-206.

Komaiko, J., & McClements, D. J. (2015). Food-grade nanoemulsion filled hydrogels formed by spontaneous emulsification and gelation: Optical properties, rheology, and stability. *Food Hydrocoll., 46*, 67-75.

685 Laemmli, U. K. (1970). Cleavage of structural proteins during the assembly of the head
686 of bacteriophage T4. *Nature, 227*, 680-685.
687 Lam, R. S., & Nickerson, M. T. (2013). Food proteins: A review on their emulsifying
688 properties using a structure-function approach. *Food Chem., 141*, 975-984.
689 Lee, S. J., & McClements, D. J. (2010). Fabrication of protein-stabilized nanoemulsions
690 using a combined homogenization and amphiphilic solvent
691 dissolution/evaporation approach. *Food Hydrocoll., 24*, 560-569.
692 Liang, T. W., Hsieh, J. L., & Wang, S. L. (2012). Production and purification of a
693 protease, a chitosanase, and chitin oligosaccharides by *Bacillus cereus* TKU022
694 fermentation. *Carbohydr. Res., 362*, 38-46.
695 Linder, M. B. (2009). Hydrophobins: Proteins that self assemble at interfaces. *Curr.*
696 *Opin. Colloid Interface Sci., 14*, 356-363.
697 Linder, M. B., Szilvay, G. R., Nakari-Setala, T., & Penttila, M. E. (2005).
698 Hydrophobins: the protein-amphiphiles of filamentous fungi. *FEMS Microbiol.*
699 *Rev., 29*, 877-896.
700 Lumsdon, S. O., Green, J., & Stieglitz, B. (2005). Adsorption of hydrophobin proteins
701 at hydrophobic and hydrophilic interfaces. *Colloids Surf. B, 44*, 172-178.
702 McClements, D. J. (2012). Nanoemulsions versus microemulsions: Terminology,
703 differences, and similarities. *Soft Matter, 8*, 1719-1729.
704 McClements, D. J., Decker, E. A., Park, Y., & Weiss, J. (2009). Structural design
705 principles for delivery of bioactive components in nutraceuticals and functional
706 foods. *Crit. Rev. Food Sci. Nutr., 49*, 577-606.
707 Paukkonen, H., Ukkonen, A., Szilvay, G., Yliperttula, M., & Laaksonen, T. (2017).
708 Hydrophobin-nanofibrillated cellulose stabilized emulsions for encapsulation
709 and release of BCS class II drugs. *Eur. J. Pharm. Sci., 100*, 238-248.

710 Peng, C., Liu, J., Zhao, D., & Zhou, J. (2014). Adsorption of hydrophobin on different
711 self-assembled monolayers: The role of the hydrophobic dipole and the electric
712 dipole. *Langmuir, 30*, 11401-11411.
713 Radulova, G. M., Golemanov, K., Danov, K. D., Kralchevsky, P. A., Stoyanov, S. D.,
714 Arnaudov, L. N., Blijdenstein, T. B., Pelan, E. G., & Lips, A. (2012). Surface
715 shear rheology of adsorption layers from the protein HFBII hydrophobin: Effect
716 of added *β*-casein. *Langmuir, 28*, 4168-4177.
717 Salis, A., Bostrom, M., Medda, L., Cugia, F., Barse, B., Parsons, D. F., Ninham, B. W.,
718 & Monduzzi, M. (2011). Measurements and theoretical interpretation of points
719 of zero charge/potential of BSA protein. *Langmuir, 27*, 11597-11604.
720 Sarparanta, M., Bimbo, L. M., Rytkonen, J., Makila, E., Laaksonen, T. J., Laaksonen,
721 P., Nyman, M., Salonen, J., Linder, M. B., Hirvonen, J., Santos, H. A., &
722 Airaksinen, A. J. (2012). Intravenous delivery of hydrophobin-functionalized
723 porous silicon nanoparticles: Stability, plasma protein adsorption and
724 biodistribution. *Mol. Pharm., 9*, 654-663.
725 Sunde, M., Pham, C. L. L., & Kwan, A. H. (2017). Molecular characteristics and
726 biological functions of surface-active and surfactant proteins. *Annu. Rev.*
727 *Biochem., 11*, 585-608.
728 Tcholakova, S., Denkov, N. D., Sidzhakova, D., Ivanov, I. B., & Campbell, B. (2003).
729 Interrelation between drop size and protein adsorption at various emulsification
730 conditions. *Langmuir, 19*, 5640-5649.
731 Tcholakova, S., Denkov, N. D., Sidzhakova, D., Ivanov, I. B., & Campbell, B. (2005).
732 Effects of electrolyte concentration and pH on the coalescence stability of *β*-
733 lactoglobulin emulsions: Experiment and interpretation. *Langmuir, 21*, 4842-
734 4855.

735 Valo, H. K., Laaksonen, P. H., Peltonen, L. J., Linder, M. B., Hirvonen, J. T., &
736 Laaksonen, T. J. (2010). Multifunctional hydrophobin: toward functional
737 coatings for drug nanoparticles. *ACS Nano, 4*, 1750-1758.
738 Xavier-Júnior, F. H., Maciuk, A., Morais, A. R. V., Alencar, E. D. N., Garcia, V. L.,
739 Egito, E. S. T., & Vauthier, C. (2017). Development of a gas chromatography
740 method for the analysis of copaiba oil. *J. Chromatogr. Sci., 55*, 969-978.
741 Yu, W., Egito, E. S. T., Barratt, G., Fessi, H., Devissaguet, J. P., & Puisieux, F. (1993).
742 A novel approach to the preparation of injectable emulsions by a spontaneous
743 emulsification process. *Int. J. Pharm., 89*, 139-146.

744

745 **Supplementary material**

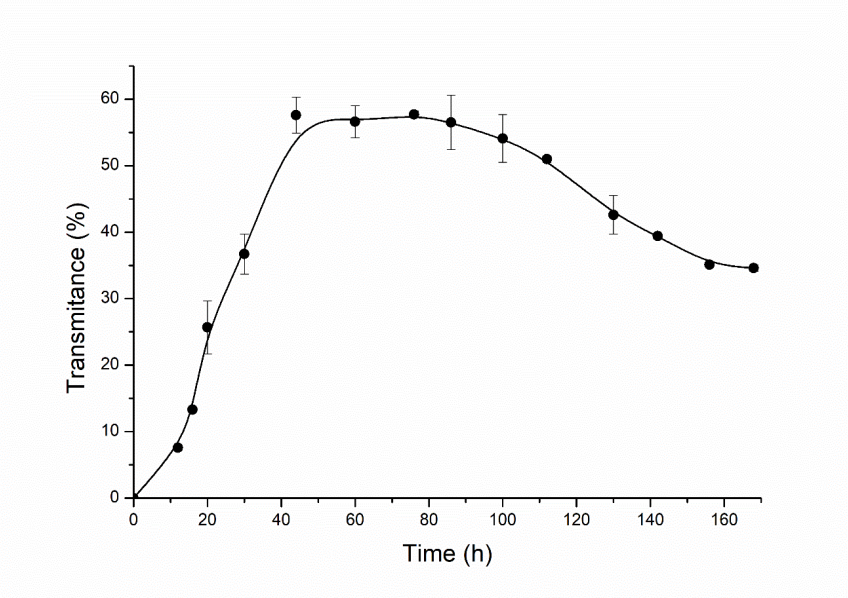


746

747 **Figure 1S -** Growth kinetics of the *T. reesei* strain by nephelometry during 7 days of
748 culture. The spores (1 x $10^5$ cells $mL^{-1}$) were obtained from 15-day-old
749 culture on potato dextrose agar (PDA) and suspended in the liquid medium
750 with lactose as carbon source. Finally, HFBII was obtained on the fourth
751 day of culture.

752

753

754

755

756

757

758

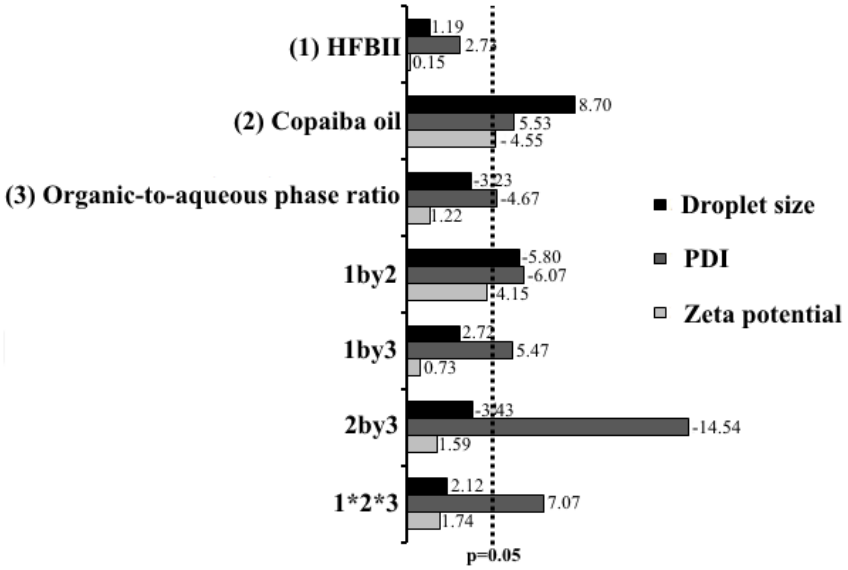


759

760 **Figure 2S-** Standardized effect of the droplet size, PDI and zeta potential performed to
761 determine the significant effects (*p*-value <0.05) responsible to produce
762 nanoemulsion systems with small values of droplet size and PDI, as well as
763 high values of zeta potential. The length of each bar in the chart indicates
764 the standardized effect of the corresponding independent variable on the
765 dependent variable. A positive or a negative sign indicates a synergistic or
766 an antagonistic effect on the dependent variable, respectively.

767

768

769

770

771

772

773

774

775 **Table 1S-** Amino acid sequences, observed and calculated molar mass and ion
776 fragments of the HFBII protein identified by MALDI-TOF MS/MS.

| Sequence | Molar mass (Da) | | Ion type |
|---|---|---|---|
| | **Obtained** | **Calculated*** | |
| **(AVCPTGLFSNP)** | 1087.52 | 1087.52 | b11 |
| **(LLCQKAIGTF)** | 1094.36 | 1093.70 | y10 |
| **(AVCPTGLFSNPLC)** | 1320.42 | 1320.64 | c13 |
| **(DQALLCQKAIGTF)** | 1433.37 | 1433.79 | x13 |
| **(AVCPTGLFSNPLCCA)** | 1449.48 | 1449.67 | a15 |
| **(VADQALLCQKAIGTF)** | 1604.32 | 1603.81 | x15 |

## 6 COMENTÁRIOS, CRÍTICAS E SUGESTÕES

**6.1** A proposta de projeto apresentada foi executada com poucas adequações e alterações. A principal mudança está relacionada com a abordagem utilizada para a determinação da formulação ótima. Inicialmente, o uso do diagrama de fases ternário foi proposto para a formulação do sistema emulsionado, o qual foi substituído, posteriormente, pelo planejamento fatorial devido às limitações de quantidade de material proteico.

**6.2** O estudo demonstrou a viabilidade do desenvolvimento de sistemas nanoemulsionados com promissora bioatividade, estabilizados por um biopolímero, através de um processo de emulsificação de baixa energia. Os resultados inéditos foram alcançados com o uso da proteína HFBII, como componente tensoativo, e o óleo de copaíba, como molécula bioativa. Os materiais e as técnicas apresentadas no artigo são explorados com o objetivo de contribuir, cientificamente, com a produção de novos sistemas carreadores, os quais poderiam ser direcionados à indústria de alimentos e de medicamentos.

**6.3** O aprofundamento e a prática do método científico se caracterizam como as evoluções intelectuais mais evidentes obtidas ao longo do mestrado.

**6.4** As metas traçadas no projeto de mestrado foram alcançadas com poucos ajustes. A perspectiva para as próximas metas, em relação à pesquisa iniciada, se refere ao aprimoramento do sistema carreador para a avaliação da sua potencial bioatividade e capacidade de transporte de moléculas.

**6.5** As perspectivas acadêmicas futuras estão relacionadas ao desenvolvimento de um projeto de doutorado, no qual haverá a integração de alunos do curso de Farmácia ao estudo para que esses possam obter conhecimentos científico e técnico.

## 7 REFERÊNCIAS


1. Araiza-Calahorra A, Akhtar M, Sarkar A. Recent advances in emulsion-based delivery approaches for curcumin: From encapsulation to bioaccessibility. Trends Food Sci. Technol. 2018;71:155-169.
2. Dickinson E. Biopolymer-based particles as stabilizing agents for emulsions and foams. Food Hydrocoll. 2017;68:219-231.
3. Sarparanta M, Bimbo LM, Rytkonen J, Makila E, Laaksonen TJ, Laaksonen P, et al. Intravenous delivery of hydrophobin-functionalized porous silicon nanoparticles: Stability, plasma protein adsorption and biodistribution. Mol. Pharm. 2012;9:654-663.
4. Balakrishnan B, Jayakrishnan A. Self-cross-linking biopolymers as injectable in situ forming biodegradable scaffolds. Biomater. 2005;26:3941-3951.
5. Khalesi M, Jahanbani R, Riveros-Galan D, Sheikh-Hassani V, Sheikh-Zeinoddin M, Sahihi M, et al. Antioxidant activity and ACE-inhibitory of class II hydrophobin from wild strain *Trichoderma reesei*. Int. J. Biol. Macromol. 2016;91:174-179.
6. Holmberg K. Natural surfactants. Curr. Opin. Colloid Interface Sci. 2001;6:148-159.
7. Sunde M, Pham CLL, Kwan AH. Molecular characteristics and biological functions of surface-active and surfactant proteins. Annu. Rev. Biochem. 2017;11:585-608.
8. Cheung DL. Molecular simulation of hydrophobin adsorption at an oil-water interface. Langmuir. 2012;28:8730-6.
9. Kallio JM, Linder MB, Rouvinen J. Crystal structures of hydrophobin HFBII in the presence of detergent implicate the formation of fibrils and monolayer films. J. Biol. Chem. 2007;282:28733-28739.
10. McClements DJ. Nanoemulsions versus microemulsions: Terminology, differences, and similarities. Soft Matter. 2012;8:1719-1729.
11. Komaiko J, McClements DJ. Food-grade nanoemulsion filled hydrogels formed by spontaneous emulsification and gelation: Optical properties, rheology, and stability. Food Hydrocoll. 2015;46:67-75.

12. Leandro LM, Vargas FS, Barbosa PC, Neves JK, Silva JA, Veiga-Junior VF. Chemistry and biological activities of terpenoids from copaiba (*Copaifera* spp.) oleoresins. Molecules. 2012;17:3866-89.
13. McClements DJ, Decker EA, Park Y, Weiss J. Structural design principles for delivery of bioactive components in nutraceuticals and functional foods. Crit. Rev. Food Sci. Nutr. 2009;49:577-606.
14. Dickinson E. Colloids in food: Ingredients, structure, and stability. Annu. Rev. Food Sci. Technol. 2015;6:211-233.
15. Anton N, Benoit JP, Saulnier P. Design and production of nanoparticles formulated from nano-emulsion templates-A review. J. Control. Release. 2008;128:185-199.
16. Salis A, Bostrom M, Medda L, Cugia F, Barse B, Parsons DF, et al. Measurements and theoretical interpretation of points of zero charge/potential of BSA protein. Langmuir. 2011;27:11597-11604.
17. Alencar EN, Xavier-Júnior FH, Morais ARV, Dantas TRF, Dantas-Santos N, Verissimo LM, et al. Chemical characterization and antimicrobial activity evaluation of natural oil nanostructured emulsions. J. Nanosci. Nanotechnol. 2015;15:880-888.
18. Khalesi M, Venken T, Deckers S, Winterburn J, Shokribousjein Z, Gebruers K, et al. A novel method for hydrophobin extraction using $CO_2$ foam fractionation system. Ind. Crop. Prod. 2013;43:372-377.
19. Araujo NK, Pagnoncelli MG, Pimentel VC, Xavier ML, Padilha CE, Macedo GR, et al. Single-step purification of chitosanases from *Bacillus cereus* using expanded bed chromatography. Int. J. Biol. Macromol. 2016;82:291-298.
20. Laemmli UK. Cleavage of structural proteins during the assembly of the head of bacteriophage T4. Nature. 1970;227:680-685.
21. Bouchemal K, Briancon S, Perrier E, Fessi H. Nano-emulsion formulation using spontaneous emulsification: Solvent, oil and surfactant optimisation. Int. J. Pharm. 2004;280:241-251.
22. Yu W, Egito EST, Barratt G, Fessi H, Devissaguet JP, Puisieux F. A novel approach to the preparation of injectable emulsions by a spontaneous emulsification process. Int. J. Pharm. 1993;89:139-146.